universität wien

MASTERARBEIT / MASTER'S THESIS

Titel der Masterarbeit / Title of the Master's Thesis

„The effect of axons of preganglionic spinal neurons on the embryonic cardiac development"

verfasst von / submitted by

Dorothea von Ahsen, BSc

angestrebter akademischer Grad / in partial fulfilment of the requirements for the degree of

Master of Science (MSc)

Wien, 2021 / Vienna, 2021

Studienkennzahl lt. Studienblatt / degree programme code as it appears on the student record sheet:	UA 066 834
Studienrichtung lt. Studienblatt / degree programme as it appears on the student record sheet:	Masterstudium Molekulare Biologie
Betreut von / Supervisor:	Univ. Prof. Dr. Tibor Harkany

Table of Contents

Acknowledgment

First I would like to thank Professor Igor Adameyko of the Department of Neuroimmunology who is always full of ideas and excitement about every possible scientific field. Thank you for taking me into your team and always having an open door to discuss my research process and prospects.

I would like to give special thanks to my mentor, Marilena Kastriti, for her dedicated supervision and unceasing encouragement throughout the development of this study. Thank you for your active support and thorough input during my writing processes, and also on the bench. With your kind and constructive feedback, you taught me to structure my thoughts and helped me on my way to become a better scientist. I feel like I am not only your apprentice, but we are colleges and friends. I am deeply grateful for your guidance, patience and friendship.

Furthermore, I would like to thank Brian Metscher, whose expertise in microCT imaging significantly contributed to this research project. Thank you for introducing this exciting field of three-dimensional imaging to me and widen my horizon to the many possibilities of interdisciplinary work in science.

I am so thankful for my family, especially my parents, and for their unconditional support and love throughout my life. I am deeply grateful for them to let me find my own way while bestowing me with security and stability. My achievements would not have been possible without them.

Finally, I want to express my profound gratitude to my partner David, and my best friends Sarah, Helena and Frederike. Thank you for all your emotional and intellectual support, for your encouraging words, and most importantly for your friendship.

Abstract

The cardiac autonomic nervous system (cANS) comprises sensory as well as sympathetic and parasympathetic motor neurons (MNs) and plays a vital role in adult cardiac function. The sympathetic division is built by preganglionic thoracic MNs synapsing onto ganglia of the sympathetic chain, which extends postganglionic adrenergic axons towards the heart. Cranial MNs traveling along the vagus nerve towards the heart form, together with cholinergic cardiac ganglia, the parasympathetic innervation. Interestingly, parasympathetic cardiac ganglia have been shown to derive from nerve-associated Schwann cell precursors (SCPs), a multipotent progeny population of the neural crest cells (NCCs); and not directly from NCCs as the majority of cANS. Preganglionic nerves are therefore crucial for the correct establishment of the cANS. In the present study, we analysed the development of cardiac innervation, in particular the temporal arrival of preganglionic nerves at the cardiac primordium and the establishment of a neurotransmitter phenotype during normal embryogenesis. Further, with the utilization of a genetic model to specifically ablate all preganglionic sympathetic visceral MNs, we investigated the role of neuronal input in cardiogenesis. We analysed the embryonic heart of this mutant strain on a structural basis with immunofluorescence and microCT imaging to elucidate whether preganglionic sympathetic MNs play a vital role for correct cardiac development. Lastly, we tested specific markers to identify different embryonic vagal sensory neuron subtypes. Our results reveal new insights essential for deciphering the crosstalk between the autonomic nervous system and embryonic cardiogenesis and further illustrates how little is known about this interaction despite a decade of research focusing on the cardiac nervous system.

Zusammenfassung

Das Herz wird durch die antagonistische Wirkung der sympathischen und parasympathischen Innervation sowie von Integration von sensorischen Nerven reguliert. Die sympathische Regulierung des Herzens stammt von präganglionischen Motorneuronen des Rückenmarks, welche Synapsen zu Ganglien des Grenzstrangs formen. Postganglionäre Axone des Stellarganglions innervieren schließlich das Herz. Parasympathische Motorneuronen, zusammen mit sensorischen Neuronen, bilden den Vagus Nerv, welcher, neben die vieler anderer Organe, auch die Funktion des Herzens kontrolliert. Axone des Vagus Nervs bilden Synapsen zu den Neuronen der intrakardinalen Ganglien. Die Neuronen dieser parasympathischen kardinalen Ganglien stammen von Schwannzell-Vorläuferzellen, welche aus der Neuronalleiste entstehen und multipotente Eigenschaften besitzen. Diese Zellen sind in engem Kontakt mit peripheren Nerven und migrieren entlang dieser zu ihrem vorgesehenen Zielort. Die korrekte Etablierung der präganglionischen Nerven ist daher essentiell für die Entwicklung des kardinalen Nervensystems. In der vorliegenden Studie haben wir die embryonale Entwicklung der kardinalen Innervation untersucht. Unser Fokus liegt auf der zeitlichen Ankunft der präganglionischen Nerven zum Herzen und die Reifung der Neuronen im Sinne der Existenz der klassischen Neurotransmitter. Wir untersuchen die neuronale Beeinflussung der Herzentwicklung mit Hilfe eines genetisch veränderten Models, in welchem die Formation aller präganglionischen Motorneuron verhindert ist. Mit dem Ziel die Bedeutung der sympathischen Innervation für die kardinale Entwicklung zu erfassen, haben wir die Morphologie des embryonalen Herzens mit Immunofloureszenz und Mikro-Computertomography Analysen untersucht. Außerdem haben wir spezifische Marker für die Identifizierung sensorischer Subtypen des Vagus Nervs analysiert. Mit dieser Studie zeigen wir deutlich, dass trotz der jahrelangen Forschung an der neuronalen Regulierung des Herzes, noch viele Details unklar sind. Unsere Ergebnisse tragen daher einen weiteren wichtigen Teil bei, die kardinalen Innervation und dessen Rolle in der Entwicklung des Säugetierherzens zu verstehen.

Introduction

Organogenesis and the Peripheral Nervous System

The unique form and function of each organ is the result of highly coordinated interaction between the processes of morphogenesis and the driving forces of cell growth, proliferation, differentiation, and death during embryonic development. Organogenesis involves coordinated growth of epithelium, mesenchyme, nerves and blood vessels, which are regulated by a wide range of genes, growth factor-signalling pathways and guidance cues (Carmeliet and Tessier-Lavigne 2005; Lammert and Cleaver 2001; Lu and Werb 2008). Because the development of organs often occurs in parallel with the development of the corresponding peripheral nerves, there are many ongoing studies investigating the roles of the autonomic innervation during organogenesis. A well-studied example for this is the crosstalk between salivary gland development and the parasympathetic submandibular ganglion (PSG). Formation of the submandibular gland (SMG), one of the major salivary glands in humans, is coincident with the maturation of neurons in the PSG (Coughlin 1975). Mouse SMG explant cultures deprived of the PSG show decreased epithelial morphogenesis and lower expression of fundamental epithelial progenitor cell markers, such as cytokeratin-5 (Knox et al. 2010). Further, parasympathetic innervation of the SMG modulates epithelial morphogenesis via the neurotransmitter acetylcholine (ACh), which activates the major muscarinic receptor in embryonic SMG epithelium, muscarinic receptor M1 (Knox et al. 2010). The G protein-coupled receptor M1 has been shown to transactivate the epidermal growth factor receptor (EGFR), independently of its principle ligands – epidermal growth factor (EGF) and transforming growth factor-α (TGF-α) (Tsai, Morielli, and Peralta 1997). Activation of EGFR leads to the activation of many downstream signalling pathways, including also a cascade of signals that maintain an undifferentiated state of epithelial progenitor cells. Therefore, acetylcholine, produced by the innervating parasympathetic neurons in the SMG, plays a key role in maintaining a pool of undifferentiated epithelial progenitor cells which is crucial during salivary organogenesis (Knox et al. 2010). The same group further revealed that parasympathetic innervation regulates tubulogenesis,

a multistep process during salivary gland development that requires coordinated proliferation, polarization and reorganization of epithelial cells to form a lumen. Temporally parallel to this, axons from the PSG migrate towards the developing end buds (Knox et al. 2010). These axons release neuronal-derived vasoactive intestinal peptide (VIP) from varicosities (nonconventional synapses), which binds to its receptor, VIPR1. This receptor is tightly clustered in SMG epithelium that undergoes tubulogenesis. Binding of VIP by VIPR1 therefore establishes further communication between neuronal and epithelial tissue. Nedvetsky et al. showed that this interaction, and not the ACh/M1 signaling, is required for correct ductal tubulogenesis. They showed that VIP activates the cAMP/PKA (cyclic adenosine monophosphate/protein kinase A) pathway which facilitates duct elongation and the subsequent formation and expansion of a single lumen (Nedvetsky et al. 2014). These studies show multiple functional key roles of parasympathetic innervation crucial for normal development of the salivary glands. Another fascinating example of the developmental dependency of autonomic innervation is the pancreas. Pancreatic islets of Langerhans, highly organized micro-organs with distinct function, shape and size, are the endocrine region of the pancreas regulating blood glucose homeostasis and islet dysfunction underlies diabetes mellitus (Asensio et al. 2005; Borden et al. 2013). The adult islets are known to be controlled by sympathetic activity (Woods and Porte 1974). However, sympathetic innervation during development has a different role. Innervation of the pancreas by sympathetic axons is dependent on the target-derived neurotrophin, nerve growth factor (NGF), and is concurred with stages of rapid growth, differentiation, and maturation in the embryonic pancreas (Glebova and Ginty 2004). By using a genetic model to ablate sympathetic innervation of the pancreas, it has been recently shown that sympathetic innervation contributes reciprocally to pancreatic organogenesis. The survival and correct innervation of sympathetic neurons depend on the signalling interaction of tropomyosin receptor kinase member TrkA and the neurotrophin NGF, which is secreted by target tissues (Glebova and Ginty 2005). Borden et al. selectively depleted TrkA protein in sympathetic neurons by crossing mice harbouring a conditional (floxed) TrkA allele with mice expressing a tyrosine hydroxylase (TH)-driven CRE recombinase, resulting in *TH-Cre;TrkA*$^{f/f}$ mutant mice. This depletion leads to the loss of sympathetic innervation of the pancreas (and several other peripheral tissues). Resulting from this ablation,

significant disruption of islet cytoarchitecture accompanied by glucose intolerance was observed in *TH-Cre;TrkA$^{f/f}$* mutant mice. Treatment with the β-adrenergic agonist isoproterenol resulted in substantial improvement in islet architecture and glucose tolerance. These results indicate that the neurotransmitter norepinephrine (NE), emitted by sympathetic innervation, acts via pancreatic β-adrenergic receptors to influence islet cell migratory behaviour in order to establish the final architecture and functional maturity of pancreatic islets (Borden et al. 2013). Peripheral nerves further play a role in the migration of precursor cells during development as they serve as delivery routes for some developing cells. Schwann cell precursors (SCPs), embryonic peripheral glial stem cells, are associated with all developing peripheral nerves. In a variety of developing tissues , SCPs detach from the innervating nerves and generate different progenitor cell types (Furlan and Adameyko 2018). One of these cell types are SCP-derived melanocytes, which inhabit not only the skin (Adameyko et al. 2009) but also the heart (Levin et al. 2009), the inner ear (Steel and Barkway 1989) and the brain meninges (Goldgeier, Klein, and Klein-Angerer 1984). Furthermore, it has been recently shown that chromaffin cells are also derived from SCPs (Furlan et al. 2017; Kastriti et al. 2019). In mammals, the two structures harbouring chromaffin cells are the adrenal medulla (AM) and the Zuckerkandl organ (ZO). Chromaffin cells are the main sources for the circulating catecholamines, including adrenaline and noradrenaline (Huber, Kalcheim, and Unsicker 2009). Catecholamines play a central role in stress-response and are fundamental during embryonic development, including normal cardiac development (Portbury et al. 2003). Fate tracing of nerve-associated SCPs using neural crest and glia-specific inducible Cre lines *Sox10^{CreERT2}* and *Plp1^{CreERT2}* coupled to the *R26R^{YFP}* reporter, showed that SOX10^{+} SCPs generate the vast majority of chromaffin cells in the AM (Furlan et al. 2017). Further, if chromaffin cells arise from SCPs, the formation of the AM should depend on nerves innervating the adrenal gland. In order to achieve ablation of preganglionic motor neurons, the genetic mouse model *Hb9^{Cre};Isl2^{DTA}* (Yang et al. 2001) was employed. Analysis of these mice revealed a selective and near complete lack of motor neurons (Yang et al. 2001) and a significant reduction of chromaffin cells in the AM (Furlan et al. 2017). Thus, the formation of the adrenal medulla depends on the nerves for delivering the precursors of chromaffin cells, the SCPs, to their destined location. This also applies for the majority of chromaffin cells in the Zuckerkandl organ

(Kastriti et al. 2019). Another progeny of the SCP population are the parasympathetic ganglia. By inducing genetic tracing in *Sox10*$^{CreERT2/+}$;*R26R*$^{YFP/+}$ animals with the administration of tamoxifen at embryonic day (E) 11.5 and analysis at E17.5 shows YFP^{+} cells in cranial parasympathetic ganglia, which shows that nerve-associated SCPs differentiate into parasympathetic neurons (Dyachuk et al. 2014). Another group revealed the dependence of cranial nerves for the correct location and formation of cranial parasympathetic ganglia by ablating major cranial nerves (Espinosa-Medina et al. 2014). Together, these findings describe the origin of the parasympathetic system, in which its neurons are recruited from SCPs, dwelling on cranial and trunk sensory and sympathetic nerves (Dyachuk et al. 2014; Espinosa-Medina et al. 2014).

With these discoveries, it becomes evident that peripheral nerves play a crucial role not only for monitoring the internal organs, but are further essential for their development. Consequently, these insights lead to the question whether there are more, yet to be discovered, interactions between the forming embryonic PNS and other developing internal organs. In this study, we wanted to investigate the potential crosstalk between peripheral nerves and the developing mammalian heart and its visceral innervation. The formation of the embryonic heart has been a topic of extensive studies, and the general mechanisms of cardiac development are well understood. However, most of these investigations were focusing on genetic (intrinsic) regulation of cell differentiation, migration and organogenesis. Simultaneously, the studies deciphering the cardiac nervous system, including the role of neurotransmitters, were mainly implemented in the adult heart. Here, I aimed to bridge cardiac innervation and cardiac development. To exemplify the necessity of the correct cardiac neuronal innervation for the function of the heart, I provide a short review of the cardiac development and its autonomic adult neuronal control.

Cardiac Development

The heart is one of the earliest organs that appear fully formed already during embryonic development. Early cardiac precursors arise from specific mesodermal progenitors that express the transcription factor *Mesp1* (Saga et al. 1999) as well as the chromatin remodelling factor SMARCD3 (Devine et al. 2014) prior to the onset of distinct

cardiac markers. These mesodermal progenitors are rapidly specified into separate cardiac cell populations around the onset of gastrulation, in mice around E6.0 to E7.5 (Devine et al. 2014). Cardiac progenitors expressing the T-box gene *Tbx5* will contribute to the left ventricle (LV) and atria (Takeuchi et al. 2003), whereas progenitors expressing the myocyte enhancer factor *Mef2c* will form the right ventricle (RV) and common outflow tract (Dodou et al. 2004). These two cell populations are also referred to as the first and secondary (or anterior) heart field, respectively. Separation of the left and right ventricles is dependent on the interventricular septum (IVS) and it has been hypothesized that the IVS myocardium is derived from both of these two heart fields (Takeuchi et al. 2003). The early segregation of the two populations suggests that the compartment boundary that exists between the right and left ventricle arises from an early clonal population, prior to the formation of the IVS morphogenesis (Devine et al. 2014). The formation of the heart tube takes place during E7.5 and E8.5 and can be divided into three phases. During the first phase, cells of the first heart field (FHF), forming the cardiac crescent, rapidly differentiate and turn into cells capable of autonomous contractions. The second phase is dominated by morphological changes, during which cell differentiation is reduced, and cells of the second heart field (SHF) migrate towards and help forming the heart tube (Ivanovitch et al. 2017). During the third phase cardiac precursor recruitment from the SHF and their differentiation resumes, contributing to the dorsal closure of the heart tube and the formation of the RV (Ivanovitch et al. 2017). Shortly after, the linear heart tube undergoes rightward looping to form an asymmetrical, curved tube (Brand 2003). The direction of the looping is evolutionary conserved and always the same in uncompromised individuals (Desgrange, Garrec, and Meilhac 2018; Jensen et al. 2013; Pérez-Pomares, González-Rosa, and Muñoz-Chápuli 2009). With the looping, lengthening of the tube and further ballooning of the future chambers lead to the first distinction of the *bulbus cordis* (future RV), primitive LV and the common atrial chamber. At E9.5 further segments can be distinguished: the atrioventricular canal connects the common atrial chamber and the primitive LV, whereas the bulboventricular canal represents the connection between the primitive LV and the future RV (Kaufman and Bard 1999). By further ballooning, the atrial chambers expand on both sides of the developing arterial pole, whereas the ventricular chambers form along the outer curvature of the ventricular loop and the IVS

forms between the two chambers (Savolainen et al. 2009). Three extracardiac cell populations are incorporated into the heart through consecutive waves of cell migration, including so called cardiac neural crest cells (CNCCs), which migrate from the dorsal neural tube down to the pharyngeal arches and then to the location of the future outflow tract. CNCCs contribute fundamentally to the septation of the common outflow tract into aortic and pulmonary channels and to the formation of the aortic arch arteries (Kirby 2007b; Yamagishi 2020).

Cardiac Innervation

Upon examination of the postnatal heart, cardiac innervation includes axons extended by sensory (afferent) as well as motor (efferent) neurons of the parasympathetic and sympathetic division of the autonomic nervous system. Adult regulation of heart rate and cardiac contraction is conducted by the cardiac autonomic nervous system (cANS) in relation with the other tissues of the cardiac conduction system (Jänig 2006; Robinson et al. 1966). Even though the development of cardiac innervation has been the subject of many investigations, the exact mechanisms navigating normal cANS development are still not known. The potential interactions of various cell types and signalling molecules involved in this process are not well understood. As described above, autonomic innervation has been found crucial for normal development of some internal organs. In our attempt to shed light on potential interplays between the cANS and cardiac development, a comprehensive revision of what is known about the development of cardiac innervation is crucial.

The cardiac sensory innervation and its development

Cardiac sensory (afferent) neurons can be functionally separated into two main groups based on whether they are associated with parasympathetic (vagal) or sympathetic nerves (Kirby 2007a). The cell bodies of the vagal sensory neurons are located in the nodose (inferior vagus ganglion) and jugular (superior vagus ganglion) ganglia and are derived from the placode and the neural crest, respectively (D'amico-Martel and Noden 1983). A recent study revealed the molecular identity of adult nodose and jugular neurons (Kupari et al. 2019). Yet, the exact intrinsic events during the development of these neurons still need to be examined. The two genes most distinctive for the adult

nodose and jugular neuron populations are *Phox2b* and *Prdm12*, respectively (Kupari et al. 2019). *Phox2b* is known to be essential for the development of cranial sympathetic (but not spinal sympathetic preganglionic neurons), parasympathetic, adrenal and enteric derivatives of the neural crest (Pattyn et al. 1999) as well as for placode-derived chemosensory neurons (Dauger et al. 2003). This gene is expressed by adult nodose cranial sensory neurons and encodes a transcription factor crucial for the maturation, survival and correct establishment of function in placode-derived peripheral sensory neurons (Kupari et al. 2019). The gene expressing PRDM12 was found to be selectively active in neural crest-derived sensory neurons, including somatosensory neural precursors in the jugular ganglia as well as in the dorsal root ganglia (DRG) (Desiderio et al. 2019). PRDM12 directs nociceptive sensory neuron development by regulating the expression of neurotrophic receptor tyrosine receptor kinase A (*TrkA/Ntrk1*), which functions to support survival, sensory subtype specification, axonal outgrowth and target-specific innervation of nociceptors (Harrington and Ginty 2013). In the present study, I used these two markers to examine the identity of the sensory vagal neurons during development. Axons of nodose and jugular neurons travel within the same nerve sheath and innervate a wide range of targets; from the skin at parts of the head to most of the visceral organs, including the heart. These nerves provide sensory information controlling both the sympathetic and parasympathetic visceral motor output (Kupari et al. 2019). The cell bodies of afferent neurons associated with the sympathetic division are residing in the dorsal root ganglia (DRG) and are derived from the neural crest (NC) (Marmigère and Ernfors 2007).

Cardiac innervation of the adult heart has been mostly mapped out, but little is known about the temporal establishment of the cardiac nervous system during embryonic development. The earliest time point at which neuronal cells have been observed is E10.5, detected by staining against the neurotrophin receptor p75 (P75NTR) for autonomic neurons (Hildreth et al. 2008). With the use of fate-tracing of neural crest-derived cells with the mouse model *Wnt1-CRE;R26Rxgal* Hildreth et al. further showed that these neuronal cells ($p75^{+}$ cells) are not NC-derived, but of other, unknown, origin. Neurofilament marker NF160D staining at E10.5 in the dorsal mesocardium confirmed the presence of nerves (possible the vagus nerve) as well as cardiac ganglia at the venous pole at this early stage. However, the study did not clarify the nature of these

neuronal fibres, whether they belong to afferent or efferent neurons. A plethora of questions regarding the origin, development and possible undiscovered roles of the sensory cardiac innervation remain. As described above, it has been recently discovered, that the vagal nerve serves as a delivery route for the precursor cells (SCPs) that later form parasympathetic ganglia, including cardiac paraganglia (Espinosa-Medina et al. 2014). Following up on this revelation, we want to investigate further roles of cardiac innervation controlling the development of cardiac ganglia and the heart itself.

The parasympathetic innervation of the heart and its development - the vagal preganglionic nerves and the paraganglia

Apart from sensory neurons, the vagal nerve comprises parasympathetic motor neurons. These preganglionic parasympathetic neurons originate in the *nucleus ambiguus* (NA) (Bieger and Hopkins 1987) and the dorsal motor nucleus of the vagus (DMV) (McLean and Hopkins 1982), both located in the *medulla oblongata* (brainstem). Their axons travel via the vagal nerve into the periphery of the body where they synapse onto postganglionic neurons of parasympathetic ganglia located in close proximity of the innervated organ. The vagal nerve extends branches to the larynx, oesophagus, lungs, aorta and the heart and their related nerve plexuses. The remaining fibres travel through the diaphragm and innervate multiple abdominal organs such as the liver, kidney, adrenal glands and the enteric system (Yuan and Silberstein 2016). As mentioned above, the vagal nerves play an essential role in the development of the cardiac ganglia (paraganglia) (Dyachuk et al. 2014; Espinosa-Medina et al. 2014). During the past few years, fascinating progress has been made in the area of embryonic precursor cells, in particular in regard to the nature of the neural crest derived SCPs (Furlan et al. 2017). SCPs are embryonic glial progenitors derived from the $FOXD3^{+}/SOX10^{+}$ migratory neural crest cells settling on the ventral and dorsal spinal roots, cranial nerves, projecting sensory, motor and visceral preganglionic motor neurons within the CNS. The transcription factor (TF) FOXD3, found in migrating NCCs, promotes glial fate while suppressing the acquisition of the alternative neuronal and melanocytic fates (as reviewed by Kastriti and Adameyko 2017). The SRY-related high-mobility-group domain transcription factors SOX10, another fundamental NC-specific TF, facilitates the specification and later maturation of SCPs towards myelinating Schwann cells.

Expression of this TF precedes neuronal differentiation and is downregulated with initiation of neurogenesis (Britsch et al. 2001). Another worth mentioning player in the differentiation of NC-derived cells into mature progeny populations is *Phox2b.* This gene has an essential role in the development of sympathetic and parasympathetic neurons (Pattyn et al. 1999). Inactivation of the gene by targeted insertion of a *LacZ* transgene which disrupts the homeobox of *Phox2b* and leads to a null phenotype, results in the complete absence of sympathetic, parasympathetic and enteric components of the autonomic nervous system in E13.5 $Phox2b^{LacZ/LacZ}$ embryos. This experiment elegantly proved the indispensability of *Phox2b* for the formation of autonomic neural crest derivatives (Pattyn et al. 1999). The expression of *Phox2b* in NC-derived cells is transient and exhibits different patterns in distinct cell populations. Many cranial nerve-associated crest cells co-express *Phox2b* together with markers of SCPs. During migration of SCPs along the nerves the expression of *Phox2b* is present, while in closer proximity to the developing organ, *Phox2b* gets switched off upon differentiation of the precursor cell into myelinating Schwann cells. In contrast, cells determined to become of neuronal nature remain expressing *Phox2b* (Dyachuk et al. 2014; Espinosa-Medina et al. 2014). SCPs exclusively migrate and proliferate along peripheral nerves and spread throughout the growing embryo together with evolving nerve innervation (Dyck et al. 2005; Jessen and Mirsky 2019). Upon maturation, the majority of SCPs develop into immature Schwann cells that later give rise to adult peripheral glial cell types (Jessen and Mirsky 2005; Kastriti and Adameyko 2017). Interestingly, SCPs retain specific molecular characteristics of NCCs and remain multipotent, making SCPs a long-lasting nerve-associated pool of neural crest-like cells (Petersen and Adameyko 2017). Remaining multipotent during embryonic development, SCPs can detach from their associated nerve fibres and convert to other cell types of the original neural crest spectrum. To this end, it is known that SCPs can give rise to melanocytes (Adameyko et al. 2009), mesenchymal stem cells (Isern et al. 2014), parasympathetic and enteric neurons (Dyachuk et al. 2014; Espinosa-Medina et al. 2014). Associated with these axons, SCPs detach from the fibres upon arrival to their destined target, amongst others, the aorta and the developing heart. With the detachment of the nerves SCPs undergo molecular transitioning and mature into peripheral glial cells or parasympathetic neurons and form cardiac ganglia (Dyachuk et al. 2014; Espinosa-Medina et al. 2014; Petersen and

Adameyko 2017). It is known, that the first axonal branches, of presumably the vagal nerve, reach the developing heart at E10.5 (Hildreth et al. 2008). But the functional roles of this early parasympathetic innervation remain to be investigated.

The sympathetic innervation of the heart and its development

The cell bodies of the visceral sympathetic preganglionic motor neurons are located in the dorsolateral region of the lateral horn of the spinal cord and are spatially separated from somatic motor neurons (Jänig 2006). In mammals, visceral motor neurons of the sympathetic preganglionic motor column (PGC neurons) known to control cardiac function arise mainly from the first three thoracic (T1 – T3) segments of the spinal cord (Markham & Vaughn 1991; Kawashima 2005). Their axons exit the spinal cord via the ventral roots and join the sympathetic chain by synapsing onto their postganglionic target neurons (Coote and Chauhan 2016). With retrograde neuronal tracing, by injecting cholera toxin subunit B (CTB) conjugated to Alexa Flour 488 into the adult mouse heart, it was recently discovered that the majority of noradrenergic sympathetic neurons innervating the heart originate in the stellate ganglion, some in the middle cervical ganglion and few in the second thoracic ganglion (Rajendran et al. 2019). At the same time, somatic and visceral preganglionic motor neurons in the spinal cord emerge from a common set of ventral progenitor cells, yet shortly after exiting the cell cycle they diversify into distinct functional subtypes (Briscoe et al. 2000). The divergence of PGC neurons and somatic motor neurons becomes apparent prior their final settling location in the spinal cord by their expression profile of distinct transcription factors (Jessell 2000). The LIM homeodomain protein pair ISL1 and ISL2 has been shown to be essential for the generation of somatic and visceral motor neurons in the spinal cord (Thaler et al. 2004). Furthermore, the homeobox gene *Hb9* is known to be crucial for the consolidation of general motor neuron identity (Arber et al. 1999). These motor neurons are known to serve as delivery routes for SCPs to the adrenal medulla (Furlan et al. 2017), which arrive at the AM and differentiate into neuroendocrine chromaffin cells. Thus, upon ablation of these nerves, in $Hb9^{Cre/+};Isl2^{DTA/+}$ mice, neuroendocrine catecholaminergic cells in the adrenal medulla are reduced (Furlan et al. 2017). Several studies showed the importance of catecholamines in the development of internal organs; especially noradrenaline/norepinephrine (NE), but also adrenaline/epinephrine

(E) and dopamine, were classified to be essential for mouse fetal development, since knockout mice lacking catecholamines, specifically NE, die starting from mid-gestation (around E12.5) (Pattyn et al. 1999; Thomas et al. 1995; Zhou et al. 1995). In this study, we wanted to investigate whether this drastic reduction of sympathetic neuron-derived catecholamines has an impact on the development of the mammalian heart. Additionally, we aimed to clarify if the preganglionic motor neurons of the spinal cord only synapse onto the ganglia of the sympathetic chain, or rather form collateral arborizing axons, which ultimately innervate cardiac postganglionic ganglia. Furthermore, cardiac parasympathetic neurons initially express elements of both adrenergic (tyroxine hydroxylase (TH) and dopamine β-hydroxylase (DBH) expression) and cholinergic (choline acetyltransferase (ChAT) expression) lineage, but adrenergic genes are down-regulated once ChAT expression is induced (Hoard et al., 2008; Weihe et al., 2005). The exact temporal regulation of these genes however is not well studied yet. Thus, the role of non-cholinergic neurotransmission by parasympathetic nerves in early embryonic stages remains unclear.

All facts stated above contribute to our knowledge about the interplay between peripheral nerves and the developing primordia of inner organs. However, many open questions still remain. This includes the morphogenetic role of early neurotransmitters and other neuromodulators released by the preganglionic and postganglionic axons and affecting the development of the heart. To summarize, in the present thesis we aim to assess the potential role of the preganglionic innervation in cardiac development, either through a direct or indirect role.

Results

Cardiac innervation during embryonic development

To validate some previously described observation stated above, regarding the temporal arrival of preganglionic nerves reaching the developing heart and lay out the groundwork for this study, I, with the help of the Adameyko lab, conducted the following experiments. Using immunofluorescent staining against neuronal markers (NF200, 2H3, PHOX2B) in whole mount and on cryosections of C57BL/6 mice we show the formation and migration of peripheral nerves at E10.5 and E11.5 (figure 1A, 1D). We detect the formation of the branches of the cranial nerves, including the cranial nerve X (vagal nerve; nX,), which already reaches the cardiac primordium at E10.5 (figure 1A and D, filled arrowhead; figure 1C and F, dotted arrowheads). We used markers for smooth muscle action (SMA) to show the aorta and the primitive heart tube, neurofilament protein 200 (NF200), which labels all developing central and peripheral nerves, and the transcription factor SOX10 to mark embryonic SCPs associated with the nerves. We detect axons exiting the spinal cord and extending to the paravertebral sympathetic chain (SC) (figure 1D). Several of these fibres appear to reach beyond the SC, eventually extending closer to internal organs and even innervating them. However, additional careful experiments have to be conducted to support this hypothesis. As expected, the $SOX10^{+}$ cells are either associated with peripheral nerves or have detached from the nerves upon arrival of their destined target site. We further proceeded with immunofluorescent detection of the same markers on cryosections (figure 1B and 1E) approximately at the level of the depicted plane in figure 1A and 1D, respectively, in order to confirm the presence of these axons proximal to the primitive heart. Due to their location, in close proximity to the right and left dorsal aorta (RDAo and LDAo, respectively), and with comparison of our whole mount data, we conclude that these axons are branches of the vagal nerve and innervate the developing cardiac primordium already by E10.5. Additionally, the presence of $SOX10^{+}/PHOX2B^{+}$ SCPs (indicated by arrow heads in figure 1C and 1F) associated with these fibres, confirms that the presumably vagal nerve serves as a delivery route for SCPs to the sites of future cardiac ganglia. Detached cells have been transitioning into a distinct cell type fate, becoming

either $SOX10^+$ glial cells or $PHOX2B^+$ neurons. To recap, these results bring the final evidence of the nature and pathway of the precursor cells of the cardiac ganglia and their dependence of peripheral nerve for migration towards their final target. With the knowledge of preganglionic innervation reaching the heart by E10.5 already, we next wanted to address the presence and potential roles of neurotransmitters, neuromodulators and other signalling molecules possibly released by these neurons.

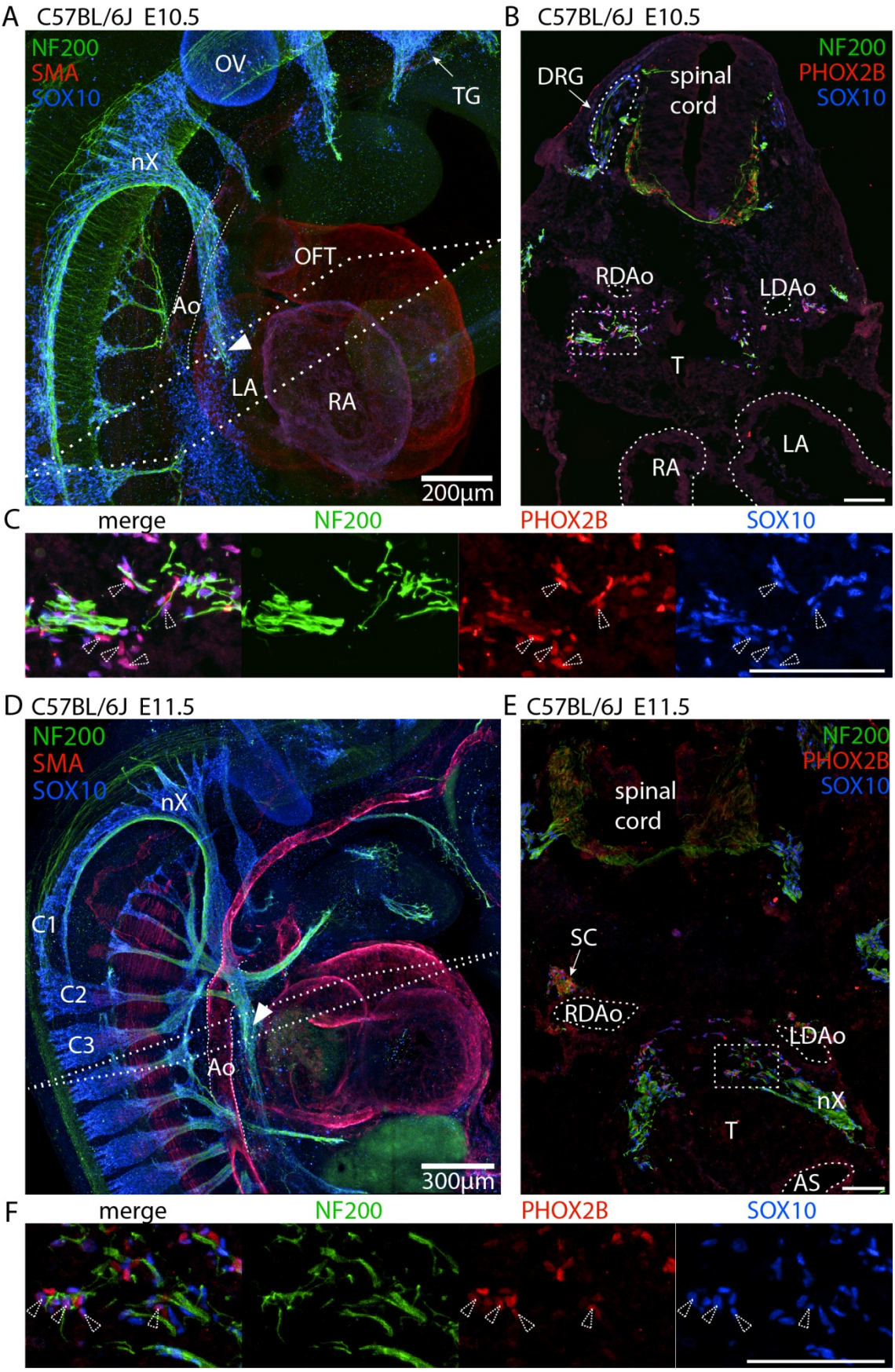
A C57BL/6J E10.5
NF200
SMA
SOX10
OV
TG
nX
OFT
Ao
LA
RA
200µm
B C57BL/6J E10.5
NF200
PHOX2B
SOX10
DRG
spinal cord
RDAo
LDAo
T
LA
RA
C
merge
NF200
PHOX2B
SOX10
D C57BL/6J E11.5
NF200
SMA
SOX10
nX
C1
C2
C3
Ao
300µm
E C57BL/6J E11.5
NF200
PHOX2B
SOX10
spinal cord
SC
RDAo
LDAo
nX
T
AS
F
merge
NF200
PHOX2B
SOX10

Figure 1. Cardiac innervation during embryonic development.

Immunofluorescence on whole mount embryos and cryosectionsof C57BL/6J embryos against NF200, PHOX2B, SMA and SOX10 show nerve fibres reaching the developing heart at E10.5 and E11.5. (**A** and **D**) Maximum projection of 3D rendering showing $SOX10^+$ SCP associated with $NF200^+$ neuronal fibres and developing heart tube with immunofluorescence against SMA in C57BL/6J mice at E10.5 and E11.5, respectively. Filled arrowhead shows vagal axons at level of cardiac primordium. (**B** and **E**) Immunofluorescence on cryosections, cross sections approximately at level of dotted plane in A and D, show vagal nerves (NF200) with associated SCPs ($SOX10^+$/$PHOX2B^+$ cells) proximal to developing primordium delivering precursor cells which later form parasympathetic cardiac ganglia. (**C** and **F**) Zoomed in area from B and E; arrowheads show double positive ($SOX10^+$/$PHOX2B^+$ cells) SCPs associated with nerve fibres. Detached cells are either $SOX10^+$/$PHOX2B^-$ or $SOX10^-$/$PHOX2B^+$. . Ao, aorta; AS, aortic sac; C1-C2, cervical (dorsal root) ganglion; DRG, dorsal root ganglia; LDAo, left dorsal aorta; LA, left atria; nX, vagal nerve; OFT, outflow tract; OV, otic vesicle; RA, right atria; RDAo, right doral aorta; SC, sympathetic chain; T, trachea; TG, trigeminal ganglion. Scale bar = 100µm (if not annotated otherwise)

Preganglionic cholinergic axons innervate forming cardiac ganglia

All preganglionic neurons of the autonomic nervous system use acetylcholine (ACh) as their primary neurotransmitter. However, the role of this neurotransmitter in the embryonic development has not been thoroughly studied yet. With the utilization of the *Chat-Cre;R26R*^{TOMATO} mouse line, we aim to determine whether preganglionic fibres innervating the cardiac ganglia, as well as postganglionic cardiac neurons themselves, already express a cholinergic phenotype at E13.5. Immunofluorescence staining against PHOX2B, *Chat*^{TOM} and 2H3 (marker for neurofilament) on sagittal cryosections of *Chat-Cre;R26R*^{TOMATO} E13.5 embryos shows cholinergic fibres innervating cardiac ganglia (figure 2C). PHOX2B labels all autonomic neurons as well as peripheral glial cells (Dyachuk et al. 2014; Espinosa-Medina et al. 2014; Pattyn et al. 1999). According to the location (in close proximity of the descending aorta and the right atrium), the great size and with consolidation of histological sections (Kaufman Atlas Plate 31a (13.5 dpc) TS 22) taken from eHistology Atlas (http://www.emouseatlas.org/eAtlasViewer_ema/application/ema/kaufman/plate_31a.php) (figure 2A), we conclude that these neuronal and partly $CHAT^+$ fibres are most likely part of the vagal nerve. The nerve further contains $CHAT^-$ axons, presumably belonging to immature neurons that either use another neurotransmitter or do not express any neurotransmitter yet. $PHOX2B^+$ parasympathetic neurons of the forming cardiac ganglia are also $CHAT^+$ already (figure 2C, solid arrowheads). We further detect $PHOX2B^+$ glial

cells (figure 2C, dotted arrowheads) located in close proximity of arborizing nerve endings. For validation of the integrity of our model, we show the expected endogenous expression pattern of *Chat*^{TOM} in spinal cord motor axons and cholinergic neurons in sympathetic chain ganglia (SCG) (figure 2D, E). Furthermore, PHOX2B is expressed in SCG neurons (figure 2E), as expected for neural crest-derived sympathoblasts (immature sympathetic neurons) (Pattyn et al. 1999). With the knowledge of preganglionic nerves innervating the cardiac ganglia expressing a cholinergic phenotype at such an early stage already, we plan to address whether this neurotransmitter and possibly other released signalling molecules affect the development of cardiomyocytes and therefore the formation of the heart with additional experiments.

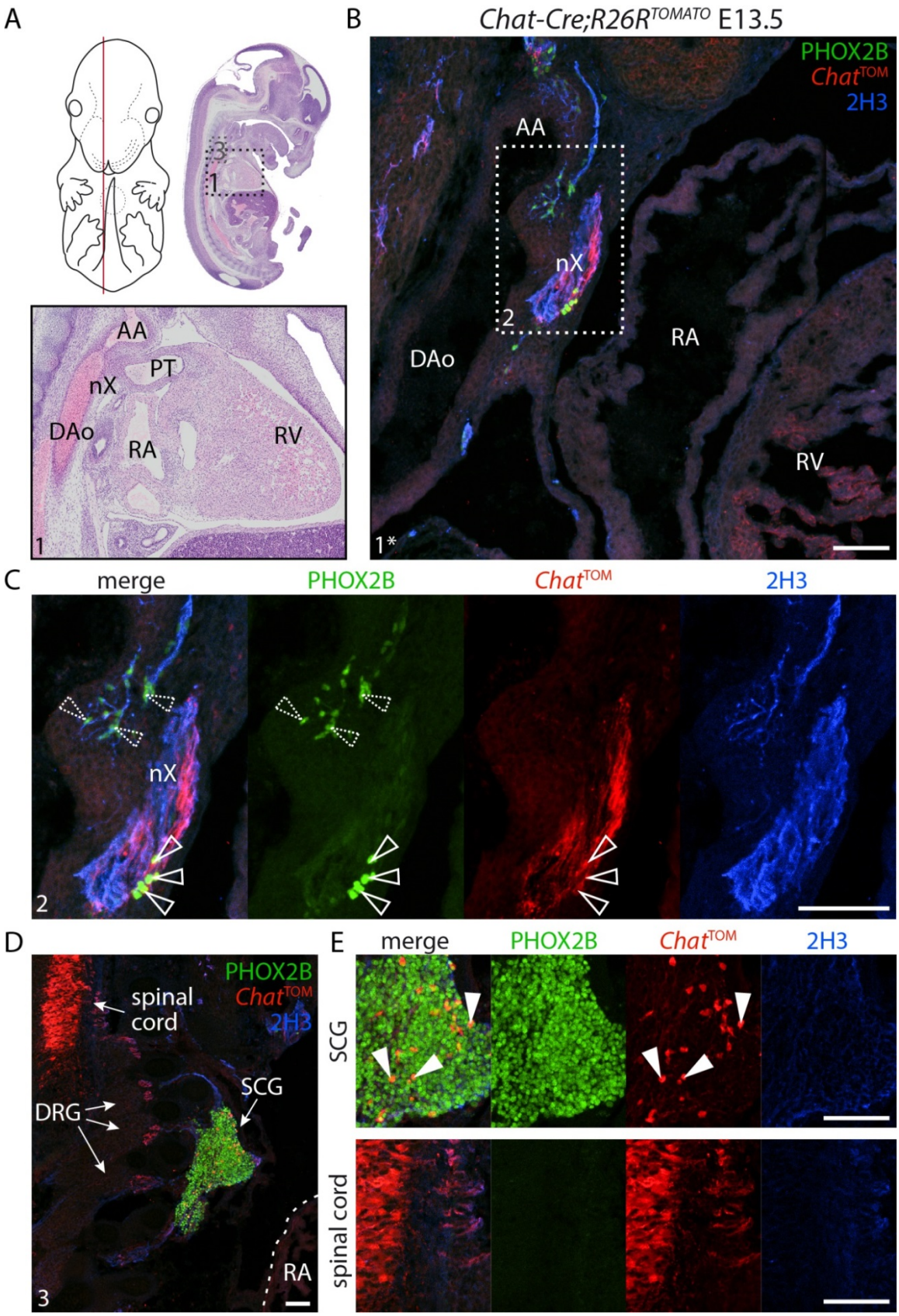
A
B
Chat-Cre;R26R^TOMATO E13.5
PHOX2B
Chat^TOM
2H3
AA
nX
RA
DAo
RV
PT
1
2
3
1*
C
merge
PHOX2B
Chat^TOM
2H3
D
E
spinal cord
SCG
DRG
SCG
spinal cord

Figure 2. Preganglionic parasympathetic *Chat*$^{TOM+}$ nerves innervate cardiac ganglia.

Genetic tracing of *Chat*$^{+}$ neurons in vicinity of the developing heart with the *Chat-Cre;R26R*^{TOMATO} mouse line at E13.5. (**A**) Schematic visualization of E13.5 mouse embryo and sagittal view of histological section of E13.5 heart. Histological section taken from eHistology Atlas (Kaufman Atlas Plate 31a, image a). (**B** to **E**) Immunofluorescence on cryosections against PHOX2B, *Chat*^{TOM}, and 2H3 in *Chat-Cre;R26R*^{TOMATO} embryos at E13.5. (**B**) Parasympathetic (*Chat*$^{TOM+}$) vagal fibres innervate developing cardiac ganglia (PHOX2B^{+} cells). (**C**) Arrowheads (solid line) show neuronal cells (PHOX2B^{+}/*Chat*$^{TOM+}$) of a cardiac parasympathetic ganglion surrounded by preganglionic innervation axons of the vagal nerve (2H3^{+}/ *Chat*$^{TOM+}$). Dotted arrowheads show PHOX2B^{+} glial cells associated with arborizing nerve endings. (**D**, **E**) Expected endogenous expression of PHOX2B in neural crest-derived sympathoblasts (immature sympathetic neurons) in the sympathetic chain ganglion (SCG). Expected expression of CHAT in mature neurons (filled arrow heads) of SCG, and in axons of the spinal cord. AA, aortic arch; Dao, descending aorta; DRG, dorsal root ganglia; nX, vagal nerve; PT, pulmonary trunk; RA, right atria; RV, right ventricle; SCG, sympathetic chain ganglion. Scale bar = 100µm.

Investigation of the cardiac ganglia in *Hb9*$^{Cre/+}$;*Isl2*$^{DTA/+}$ embryos

To assess the role of preganglionic nerves in cardiac development, we used the *Hb9*$^{Cre/+}$;*Isl2*$^{DTA/+}$ (Yang et al. 2001) mouse model to specifically ablate preganglionic visceral motor neurons. For this a *Hb9*^{Cre} mouse line, which expresses Cre recombinase selectively in motor neurons, was crossed with an *Isl2*^{DTA} mouse line in which a diphtheria toxin (DTA) gene, preceded by an IRES-loxP-stop-loxP sequence (Lee et al. 2000), had been inserted into the 3´ UTR of the *Isl2* gene. In *Hb9*^{Cre};*Isl2*^{DTA} mice, the translational stop sequence found upstream from the DTA coding region is deleted selectively in motor neurons, driving the expression of DTA when motor neurons exit the cell cycle. Analysis of these mice from E12.5 to E18.5 revealed a selective and near complete lack of all spinal motor neurons (Yang et al. 2001), as well as a significant reduction of chromaffin cells in the AM (Furlan et al. 2017). As described before, we could confirm that adrenergic cells of the adrenal medulla (AM) are significantly decreased in *Hb9*$^{Cre/+}$;*Isl2*$^{DTA/+}$ mice (figure 3E), leading to a systemic decrease of circulating catecholamines in the whole embryo (Furlan et al. 2017). Staining against cocaine and amphetamine regulated transcript (CART) and tyrosine hydroxylase (TH) enables the visualization of sympathoblasts, while also visualizing chromaffin cells TH+/CART^{-}(Chan et al. 2016). We further analysed the sympathetic chain and could not detect a significant phenotype in the adrenergic neurons (CART+/TH^{+}) of the sympathetic chain ganglia (SCG) (figure 3D, right panel). This was to be expected, since

the SCGs are NC-derived (Le Douarin and Kalcheim 1999), and not dependent on preganglionic nerves for the precursor cells to arrive at their destined location. Our main interest was focusing on the formation of the cardiac ganglia. We were interested if the cardiac ganglia depend on trophic support of the preganglionic neurons of the spinal cord. Staining against PHOX2B, PGP.5 and TH on cryosections in *Isl2*$^{DTA/+}$ E14.5 mice shows cardiac ganglia in the expected locations dorsally of the developing atria (future right and left atria) and ventrally of the primary bronchi (figure 3A and 3B, left panel). We detect normally developed cardiac ganglia located at the same sites on cryosections in *Hb9*$^{Cre/+}$;*Isl2*$^{DTA/+}$ E14.5 mice (figure 3C and 3D, left panel). Therefore, we can conclude that the presence of visceral motor neurons is dispensable for the correct establishment of cardiac paraganglia. Additional analyses of the cardiac morphology were required to allow for a concrete statement about the significance of visceral motor neurons and the decrease of catecholamines influencing the cardiac development.

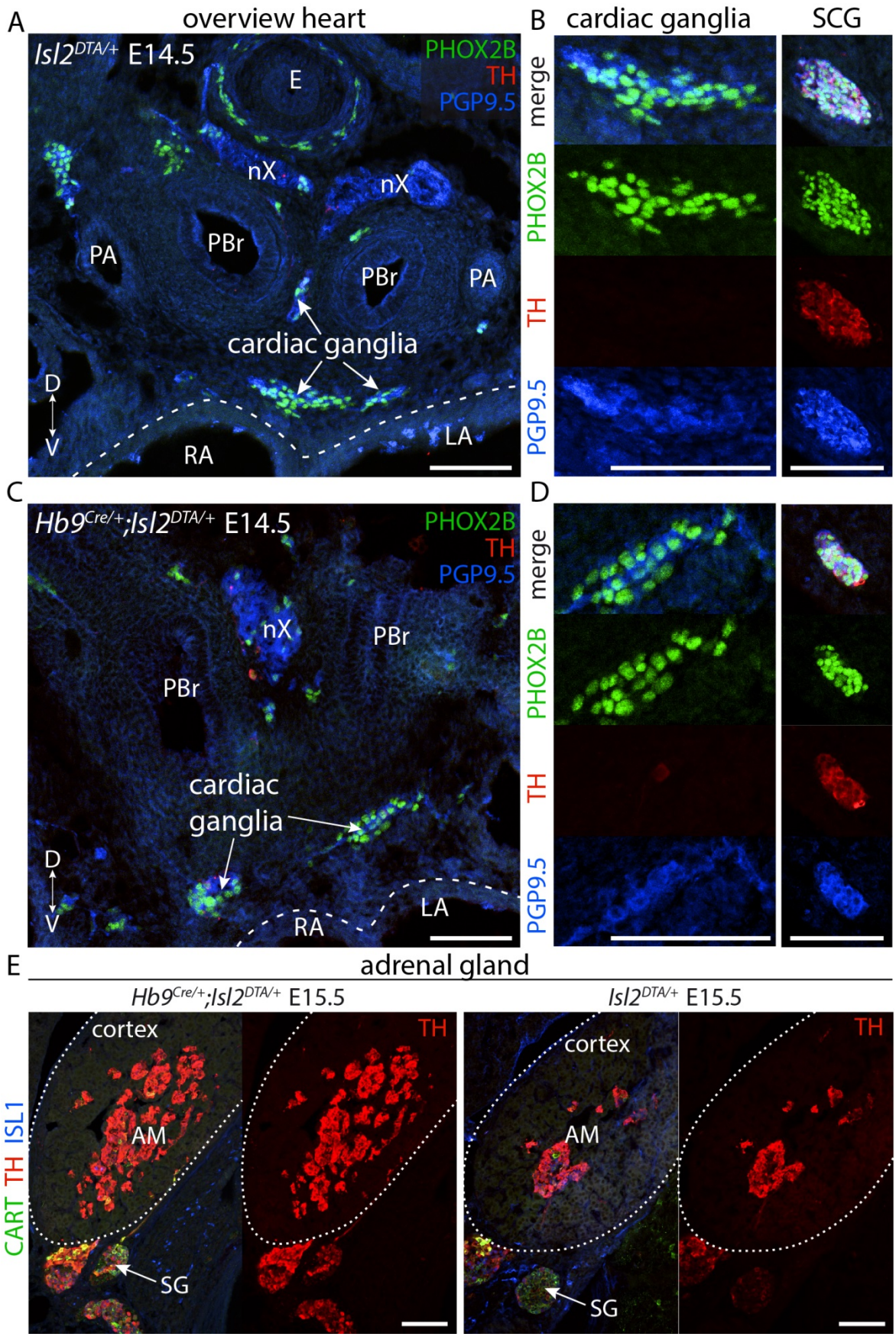
A
overview heart
Isl2DTA/+ E14.5
PHOX2B
TH
PGP9.5
E
nX
nX
PA
PBr
PBr
PA
cardiac ganglia
D
V
RA
LA
B
cardiac ganglia
SCG
merge
PHOX2B
TH
PGP9.5
C
Hb9Cre/+;Isl2DTA/+ E14.5
PHOX2B
TH
PGP9.5
nX
PBr
PBr
cardiac
ganglia
D
V
RA
LA
D
merge
PHOX2B
TH
PGP9.5
E
adrenal gland
Hb9Cre/+;Isl2DTA/+ E15.5
Isl2DTA/+ E15.5
CART TH ISL1
cortex
TH
AM
SG
cortex
TH
AM
SG

Figure 3. Cardiac ganglia in *Hb9*$^{Cre/+}$*Isl2*$^{DTA/+}$show no aberrant phenotype.

(A to D) Immunofluorescence on cryosections in *Isl2*$^{DTA/+}$ and *Hb9*$^{Cre/+}$;*Isl2*$^{DTA/+}$ E14.5 mice at level of trachea bifurcation into primary bronchi against PHOX2B, TH and PGP9.5 show presence of cardiac ganglia at predicted locations. (D) Cardiac ganglia appear to develop normally; and adrenergic neurons of sympathetic chain (SC) show no alterations in cell number or expression of TH in *Hb9*$^{Cre/+}$;*Isl2*$^{DTA/+}$ mice. (E) Immunofluorescence on cryosections in *Isl2*$^{DTA/+}$ and *Hb9*$^{Cre/+}$;*Isl2*$^{DTA/+}$ E15.5 mice at level of adrenal medulla against CART, TH and ISL1 show a decrease in TH^{+} sympathetic neurons in *Hb9*$^{Cre/+}$;*Isl2*$^{DTA/+}$ mice. Scale bar = 100µm. D, dorsal; V, ventral. AM, adrenal medulla; E, oesophagus LA, left atria; nX, vagal nerve; PA, pulmonary artery; PBr, primary bronchi; RA, right atria

MicroCT analysis and 3D segmentation of *Hb9*$^{Cre/+}$;*Isl2*$^{DTA/+}$ E18.5 hearts

After addressing the formation of cardiac paraganglia, we subsequently investigated the gross anatomy of cardiac structures in *Hb9*$^{Cre/+}$;*Isl2*$^{DTA/+}$ embryos. In light of the absence of almost all visceral motor neurons and decrease in circulating catecholamines, we reasoned that either of these phenotypes in the mutants can cause possible malformation of the embryonic heart. Because of the late developmental stage at which we chose to analyse the heart (E18.5) whole mount immunofluorescence methods were not applicable. In order to obtain three-dimensional (3D) images with preserved volumetric relations, we used tomographic imaging methods (micro computer tomography; microCT) and subsequent 3D reconstruction of the scans. Depicted in figure 4, we show representative examples of the control (*Isl2*$^{DTA/+}$) and the mutant (*Hb9*$^{Cre/+}$;*Isl2*$^{DTA/+}$) hearts in the contracted cardiac state. To ensure a qualitative comparison of the cardiac anatomical structures, we further chose three (sagittal, cross and transverse) planes at distinct levels. We can see the normal asymmetry of the ventricles, the right ventricle being distinctively smaller than the left, in almost all of the control *Isl2*$^{DTA/+}$ hearts (figure 4C, D). In contrast, some mutant *Hb9*$^{Cre/+}$;*Isl2*$^{DTA/+}$ hearts show a less clear left-right asymmetry (figure 4G, H). Furthermore, the width of the interventricular septum (IVS) appears to be decreased in relation to the ventricular walls in *Hb9*$^{Cre/+}$;*Isl2*$^{DTA/+}$ hearts (figure 4G, H). Another possible phenotype in the *Hb9*$^{Cre/+}$;*Isl2*$^{DTA/+}$ hearts concerns atrial development. As visible in the 3D volume rendering in figure 4E, the atrial appendages of some *Hb9*$^{Cre/+}$;*Isl2*$^{DTA/+}$ hearts appeared to be malformed and smaller in size compared to *Isl2*$^{DTA/+}$ hearts. However, we did not

include the analysis of the atrial structures in this study. Below I discuss the exclusion of this analysis in more detail (refer to “Discussion”).

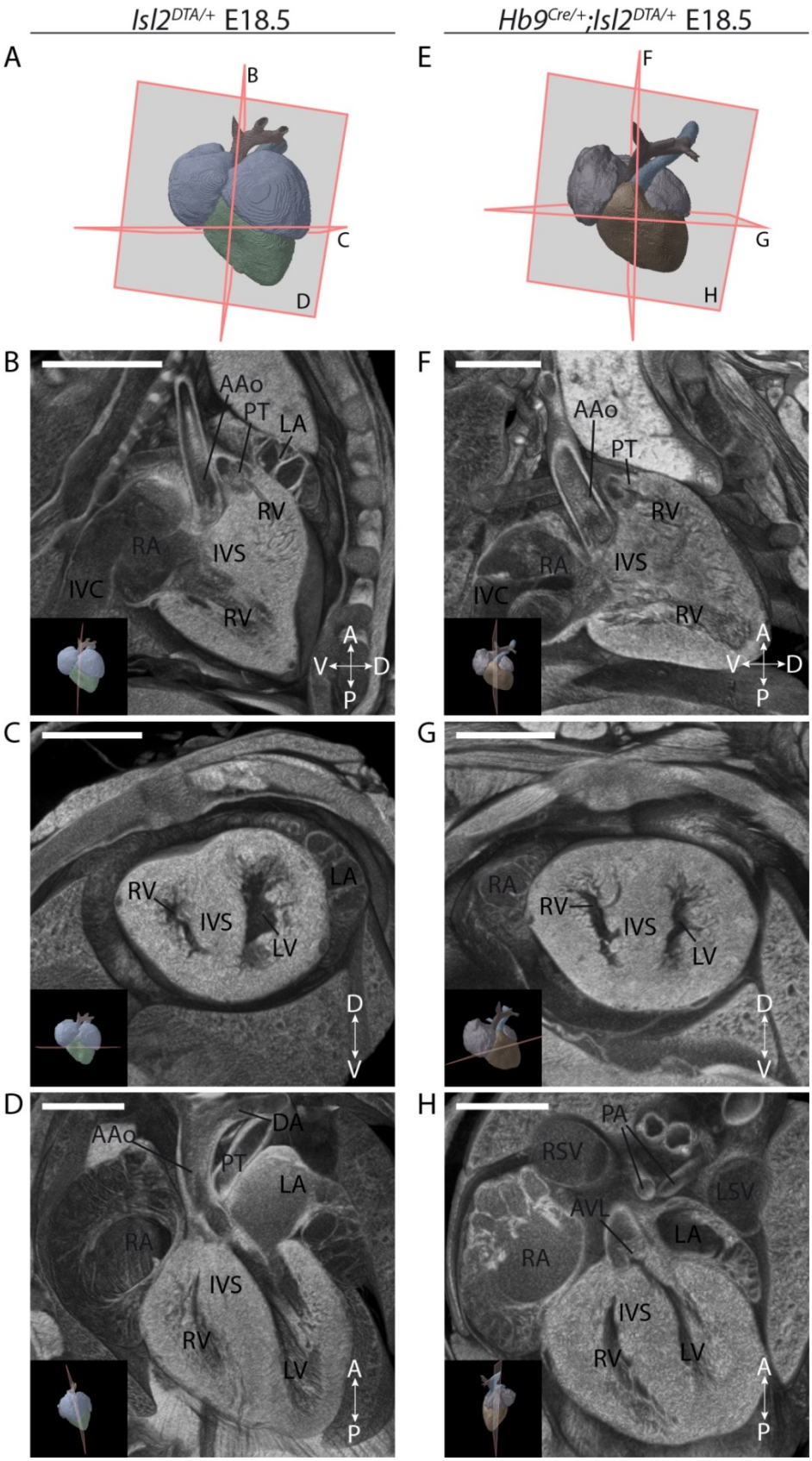

Figure 4. MicroCT images of *Hb9*$^{Cre/+}$;*Isl2*$^{DTA/+}$ embryonic heart at E18.5 show aberrant left-right asymmetry of the ventricles and decreased volume of the interventricular septum.

Representative microCT images and 3D volume renderings constructed by segmentation of *Isl2*$^{DTA/+}$ and *Hb9*$^{Cre/+}$;*Isl2*$^{DTA/+}$ mouse heart at E18.5 in the contracted state. The reconstructed voxel size for these images is 5µm. (**A**, **E**) 3D illustration of embryonic heart (constructed by segmentation with the 3D Visualization & Analysis Software Amira-Avizo) demonstrating the planes corresponding to the sites view in B-D and F-H. (**A** to **H**) 3D reconstructed volume rendering (A, E) and 2D planes of sagittal (B, F), cross (C, G) and transverse (D, H) sections of a *Isl2*$^{DTA/+}$ and *Hb9*$^{Cre/+}$;*Isl2*$^{DTA/+}$ heart, respectively. Interventricular septum (IVS) appears to have less relative volume in *Hb9*$^{Cre/+}$;*Isl2*$^{DTA/+}$ embryos (G), when compared to the IVS of *Isl2*$^{DTA/+}$ embryos (C). Asymmetry of the left and right ventricle is less distinct in *Hb9*$^{Cre/+}$;*Isl2*$^{DTA/+}$ embryos (H) than in the control (D). A, anterior; D, dorsal; P, posterior; V, ventral. Aao, ascending aorta; IVC, inferior vena cava; IVS, interventricular septum; LA, left atria; LV, left ventricle; PT, pulmonary trunk; RA, right atria; RV, right ventricle. Scale bar = 1000µm.

In order to fill, empty and refill with the circulating blood, the heart undergoes a constant cycle of muscular contraction and relaxation. This cardiac cycle can be divided into ventricular and atrial systole (contraction) and diastole (relaxation) (Katz 2011). For simplification, we only focused on the ventricular conformation and categorized the samples into contracted and relaxed ventricular state. This is necessary since the appearance of the heart changes with contraction and relaxation of the muscle cells. After dividing the samples into contracted or relaxed states, the observations regarding the decreased asymmetry are even more visible when looking at the heart in the relaxed state (figure 5D). Nevertheless, quantitative analysis of the ventricular volumes displayed inconclusive results. When analysing all samples of each genotype, the naturally induced volumetric changes during the cardiac cycle become evident (figure 5F). This supports our approach to separate the samples according to their cardiac state. However, several samples of both genotypes revealed to have a larger right ventricle than the left (figure 5E, F). Even though, after determining the ratio of the left and right ventricle (LV/RV), it was visible, that the asymmetry between left and right is less distinct in mutant *Hb9*$^{Cre/+}$;*Isl2*$^{DTA/+}$ hearts (figure 5G). To quantitatively support our hypothesis of a hypotrophic interventricular septum (IVS), we also measured the volume of the IVS by segmenting septum from the most apical to the most basal point where the ventricular wall connects to the septum. In order to bypass the overall size differences between the samples, we normalized the IVS volume with the total ventricular volume. Upon qualitative analysis, the myocardium of the IVS in mutant *Hb9*$^{Cre/+}$;*Isl2*$^{DTA/+}$ hearts

appears to have less volume in relation to the ventricular myocardium compared to control *Isl2*$^{DTA/+}$ hearts; the mean of the normalized volume of IVS in mutant mice is lower compared to the mean volume of the IVS in the control mice (figure 6A, B). However, neither analysis showed a statistical significance. This might be due to the small sample size and the natural variation of size and developmental progression between embryos (which has been reported to be the case in mice even within the same litter). Furthermore, by separation of the samples into contracted and relaxed state, the samples size (per state and genotype) was further decreased. To gain more information adding to the comprehension of the observed phenotype, we finally investigated the total ventricular volume and observed an overall smaller volume in the mutant *Hb9*$^{Cre/+}$;*Isl2*$^{DTA/+}$ hearts (figure 6C, D). However, in both the control and mutant groups we see a great volumetric range in the ventricular myocardium. We conclude that the mutation in *Hb9*$^{Cre/+}$;*Isl2*$^{DTA/+}$ mice, leading to the ablation of spinal motor neurons and furthermore a systemic decrease of circulating catecholamines, affects the cardiac and in particular the ventricular development. However further investigations have to be conducted in order to gain full understanding of the causes and effects leading to this phenotype.

Variation of cardiac phenotype in control and mutant mice

With the observed variation between each sample, we were interested to acquire a greater overview of the overall, three-dimensional structure of the embryonic heart. After the analyses described above, we created a three-dimensional atlas of all samples by segmentation and 3D-reconstruction of all cardiac structures, including also the ascending aorta, the aortic arch, and the pulmonary trunk. Figure 7 shows all samples, sorted by genotype and further categorized into contracted and relaxed cardiac state. Not only can the ventricular contraction and relaxation can be distinctively detected by this visualization, but it further shows how the structure of the atrial appendages varies due to the atrial systole and diastole. We can further observe a great variation within the same cardiac state and genotype regarding the relative size of the ventricles and the atria. This was an effort to recapitulate the developmental variation that is expected, especially since embryonic mouse development is asynchronous within the same litter.

This variation could potentially be masking the differences between the genotypes. A greater sample size is therefore necessary to compensate for this naturally occurring variation and allow for a significant and detailed statement about the cardiac phenotype in the *Hb9*$^{Cre/+}$;*Isl2*$^{DTA/+}$ strain.

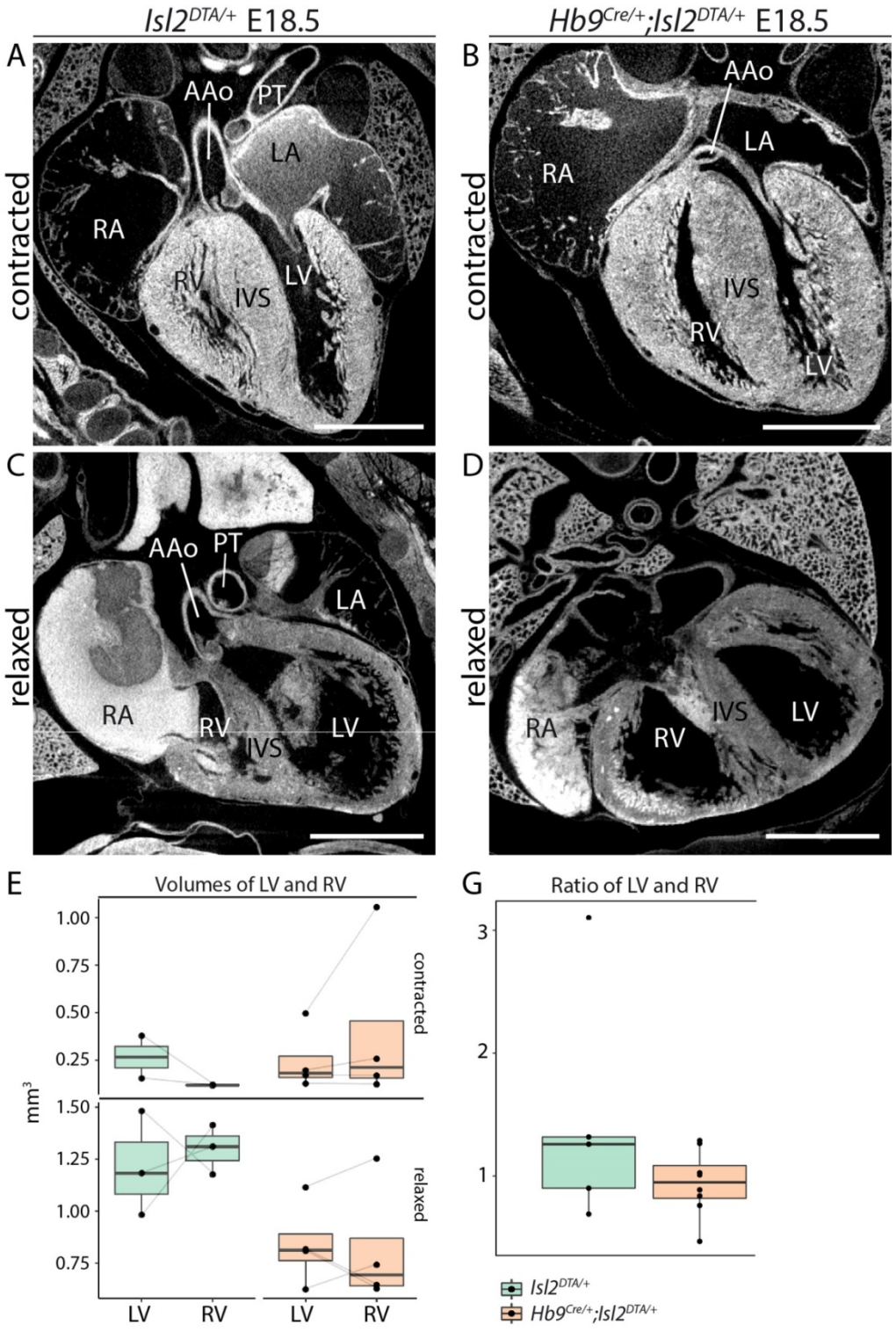

Figure 5. MicroCT images of *Hb9*$^{Cre/+}$;*Isl2*$^{DTA/+}$ embryonic heart at E18.5 in contracted and relaxed state and analysis of the asymmetry ratio of the left and right ventricle.

Representative microCT images of *Hb9*$^{Cre/+}$;*Isl2*$^{DTA/+}$ mouse heart at E18.5 in the contracted and relaxed state. Transverse section approximately at level of aorta entering left ventricle. (**A**, **B**) Embryonic heart in contracted state in *Isl2*$^{DTA/+}$ (A) and *Hb9*$^{Cre/+}$;*Isl2*$^{DTA/+}$ (B). (**C**, **D**) Embryonic heart in relaxed state in *Isl2*$^{DTA/+}$ (C) and *Hb9*$^{Cre/+}$;*Isl2*$^{DTA/+}$ (D). (**E**, **F**) Volumes of the left and right ventricle were measured by segmentation of the inner cavity of the ventricles with the 3D Visualization & Analysis Software Amira-Avizo. Volumetric analysis of the left and right ventricle, samples divided into the contracted and relaxed state (E), and all samples together (F); y-axis is in mm^3. (**G**) Ratio of the volumes of the left and right ventricle (LV/RV). Statistical analysis is shows no significance because the power of samples (*Isl2*$^{DTA/+}$ n=5; *Hb9*$^{Cre/+}$;*Isl2*$^{DTA/+}$ n=8) is too low . Scale bar = 1000µm.

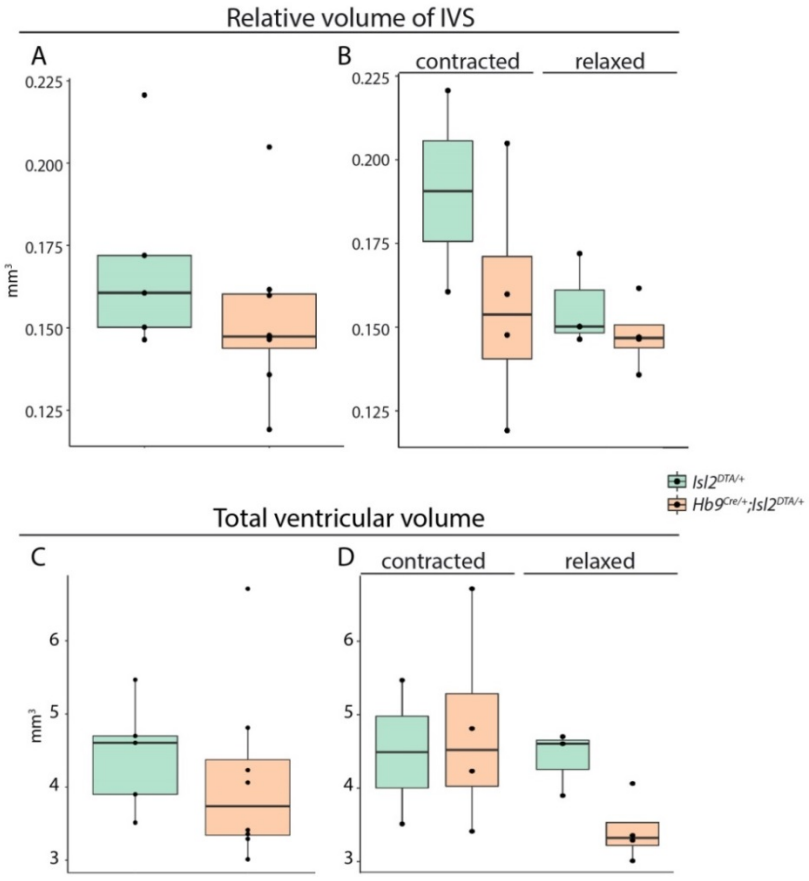

Figure 6. Volumetric analysis of total ventricular myocardium and relative volume of interventricular septum.

Values of the relative volume of IVS (normalized by the total ventricular volume) and total ventricular myocardium (ventricular walls and interventricular septum; IVS) were obtained by segmentation of the respective structures with the 3D Visualization & Analysis Software Amira-Avizo. (**A**, **B**) Relative volumes of the interventricular septum (IVS) of the *Isl2*$^{DTA/+}$ and *Hb9*$^{Cre/+}$;*Isl2*$^{DTA/+}$ hearts in contracted and relaxed state. The volumes of the IVS were normalized by the volume of the total ventricular volume. IVS volume of *Hb9*$^{Cre/+}$;*Isl2*$^{DTA/+}$ is smaller than in *Isl2*$^{DTA/+}$ hearts. (**C**, **D**) Total ventricular myocardium of the *Hb9*$^{Cre/+}$;*Isl2*$^{DTA/+}$ hearts is decreased in comparison to *Isl2*$^{DTA/+}$ embryos. Statistical analysis is shows no significance because the power of samples (*Isl2*$^{DTA/+}$ n=5; *Hb9*$^{Cre/+}$;*Isl2*$^{DTA/+}$ n=8) is too low.

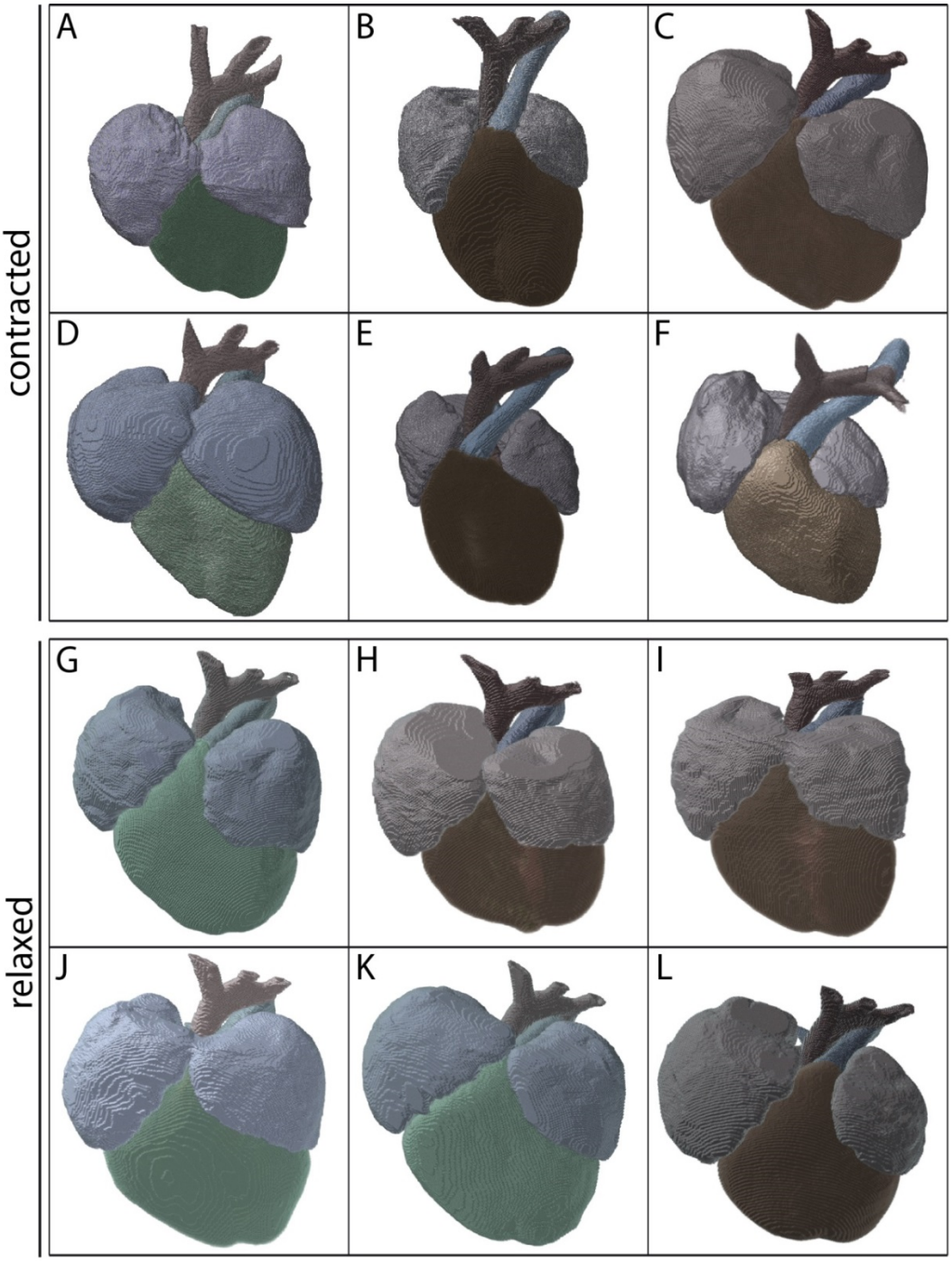

Figure 7. 3D volume rendering of *Isl2*$^{DTA/+}$ and *Hb9*$^{Cre/+}$;*Isl2*$^{DTA/+}$ embryonic hearts at E18.5 show natural variance of cardiac structure.

Three-dimensional rendering of all analysed embryonic hearts from of *Isl2*$^{DTA/+}$ and *Hb9*$^{Cre/+}$;*Isl2*$^{DTA/+}$ mice. Hearts are categorized into being contracted (**A** to **F**) or relaxed (**G** to **L**). *Isl2*$^{DTA/+}$ hearts are visualized with green ventricles (**A**, **D**, **G**, **J** and **K**); *Hb9*$^{Cre/+}$;*Isl2*$^{DTA/+}$ hearts are visualized in brown (**B**, **C**, **E**,**F**, **H**, **I** and **L**).

Development of sensory vagal neurons in the jugular and nodose ganglia and identification of specific markers

To demarcate the cardiac innervation, including also the vagal sensory neurons innervating the heart, we further investigated previously described markers specific for adult sensory neurons of the vagus nerve. The sensory compartment of the vagal nerve originates in the nodose and jugular ganglia (Berthoud and Neuhuber 2000) and comprises several different sensory subtypes such as mechano- and chemosensitive as well as nociceptive types (Kupari et al. 2019; Marmigère and Ernfors 2007). Few studies indicate that sensory vagal neurons that innervate the heart solely originate in the nodose ganglion (Chang et al. 2015; Kupari et al. 2019; Marmigère and Ernfors 2007). Further, the vagal nerve is comprised not only of sensory neurons but also harbours axons of parasympathetic preganglionic motor neurons originating in the brain stem (Bieger and Hopkins 1987; McLean and Hopkins 1982). It is therefore crucial to find reliable molecular markers for demarcating nodose and jugular sensory as well as motor neurons, in order to distinguish which neuron types innervate the heart during murine embryonic development. To do this, we applied third-generation in situ hybridization chain (Hybridization Chain Reaction - HCR) reaction in whole embryos and immunofluorescent detection on cryosections against two known markers for the adult sensory vagal neurons, located in the jugular and nodose ganglia. For now, the molecular identity of these cell populations has been described only in adult mice (Kupari et al. 2019; Wang et al. 2017). Using HCR against the genes *Phox2b* and *Prdm12* in E13.5 C57BL6/J mice, we show that these genes are selectively expressed by either nodose or jugular embryonic neurons. *Phox2b* is solely expressed by sensory neurons of the nodose ganglion, whereas *Prdm12* expression is only found in jugular afferent neurons (figure 8A and 8B). We see expression of both genes in other expected structures (figure 8C, overview), which confirms the integrity of our results. Specifically, neurons in the trigeminal ganglion (TG) and dorsal root ganglia (DRG) are positive for *Prdm12* (figure 8C, first inset) (Desiderio et al. 2019). Additionally, for the correct detection of *Phox2b*, we show the endogenous expression of neurons in the brain stem, specifically parasympathetic motor axons, which bypass the vagal sensory ganglia (figure 8C, second inset) (Pattyn et al. 1999). To further validate our results, we consolidated

data from Allen Developing Mouse Brain Atlas (2008), which shows the same expression pattern for *Prdm12* and *Phox2b* (figure 8E and E´). With our results, we can confirm the utility of these markers to employ transgenic mouse lines for targeted ablation or tracing of specific vagal sensory neurons during development.

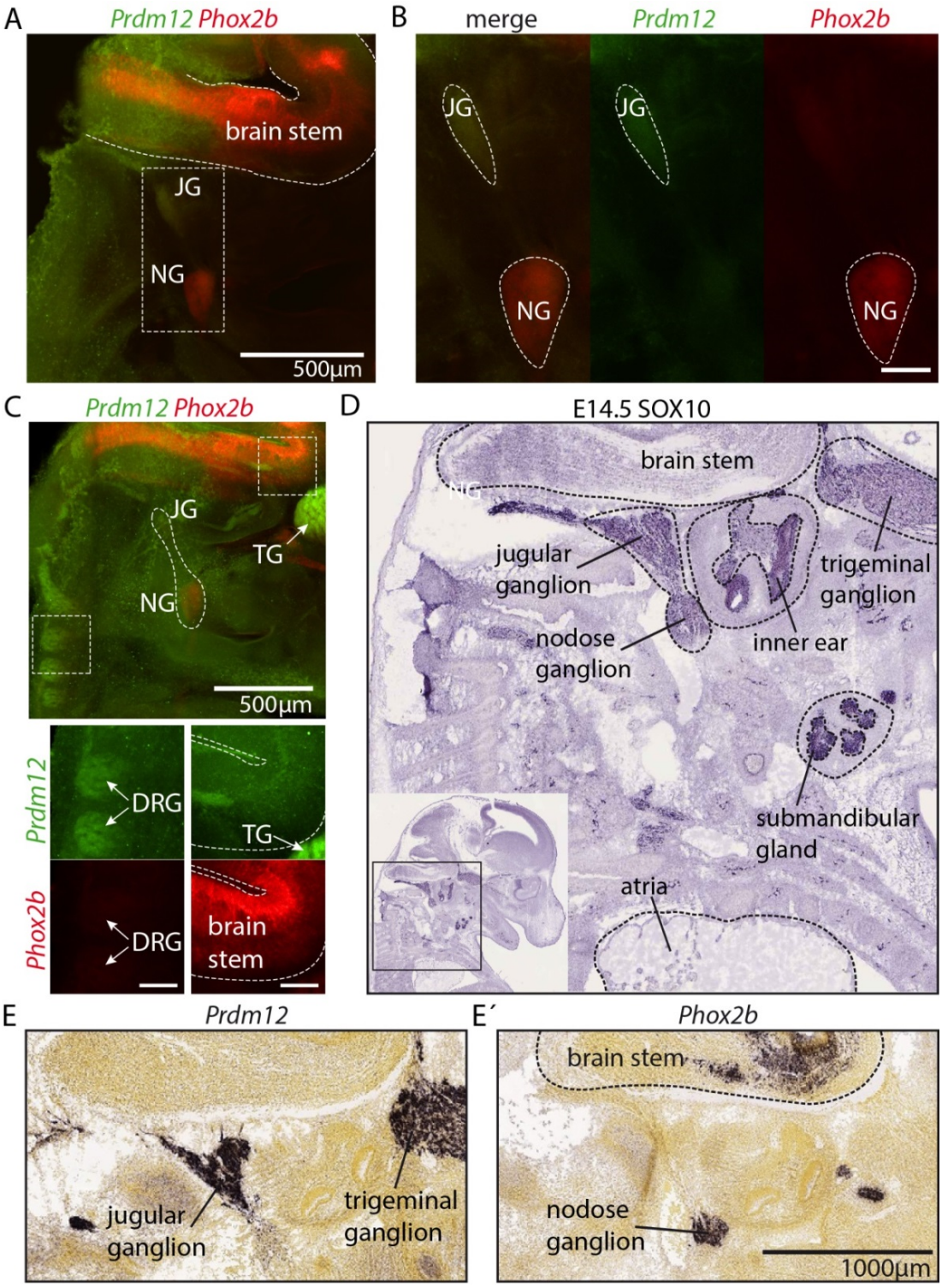

Figure 8. Embryonic nodose and jugular ganglia express distinct genes.

(A to C) Hybridization Chain Reaction (HCR) against *Prdm12 a*nd *Phox2b* in C57BL6/J E13.5 embryos. (A) Overview of embryonic jugular and nodose ganglion and the brain stem. (B) *Prdm12* is exclusively expressed by the neurons of the jugular ganglion; *Phox2b* is only expressed by nodose neurons. (C) Endogenous expression of *Prdm12* by neurons of the DRG and the trigeminal ganglion; expression of *Phox2b* by neurons located in the brain stem. (D) Overview of cranial structures at level of vagal ganglia. (E and E´) In situ against *Prdm12 a*nd *Phox2b* in E13.5 C57BL6/J embryos. Scale bar = 100µm (if not annotated otherwise). DRG, dorsal root ganglia; JG, jugular ganglion; NG, nodose ganglion; TG, trigeminal ganglion. Image credit for D and E: Allen Developing Mouse Brain Atlas (2008), see hyperlinks under "References".

With immunofluorescence on cryosections against ISL1 and *Phox2b*^{TOMATO} in *Phox2b-Cre;R26R*^{TOMATO} E13.5 embryos (figure 9) we further affirm our results described above. Nearly all general sensory neurons express the pan-sensory homeodomain transcription factor Islet1 (*Isl1*) (Anderson 1999; Yang et al. 2008), which makes it a reliable marker to detect sensory neurons. We detect ISL1^{+}/*Phox2b*$^{TOMATO+}$ cells solely located in the nodose ganglion (figure 9B, indicated by arrowheads). As expected, axons of cranial motor neurons originating in the brain stem are also *Phox2b*$^{TOMATO+}$ (Pattyn et al. 1999). Confirming the usability of these markers to distinguish different neuronal types of the vagus nerve allows us and fellow researchers to further investigate the innervation targets of the vagus nerve by staining, tracing or ablating distinct neuron populations.

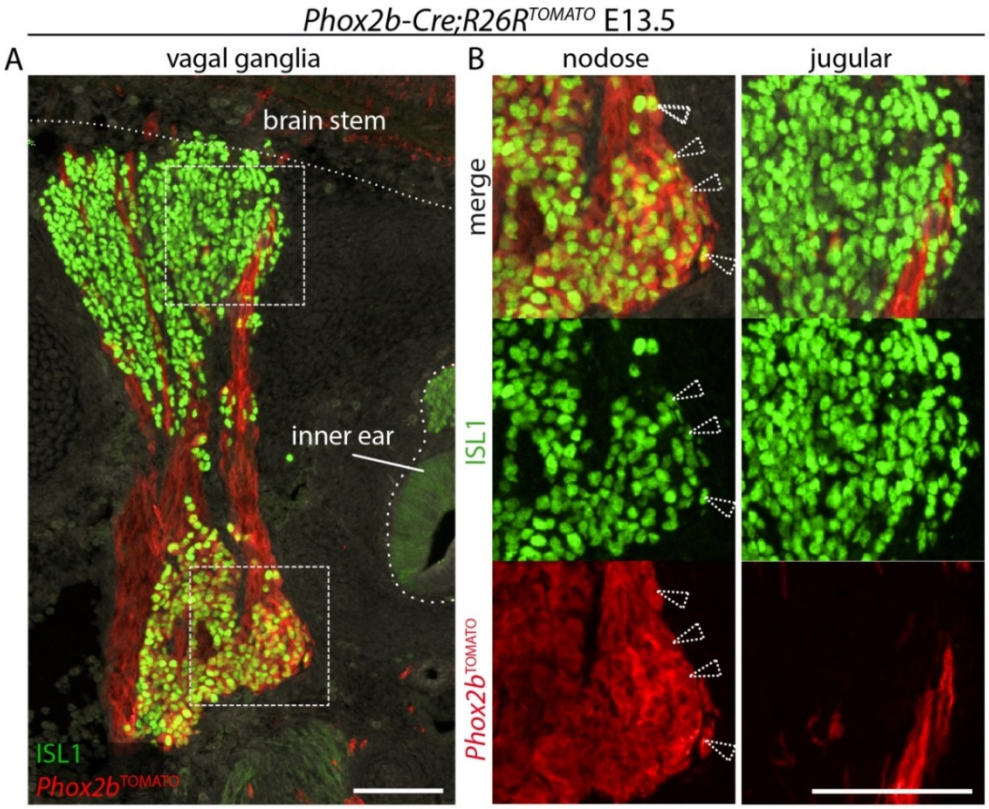

Figure 9. PHOX2B is expressed in embryonic nodose neurons.

(A and B) Immunofluorescence on cryosections (sagittal) against ISL1 and *Phox2b*^{TOMATO} in *Phox2b-Cre;R26R*^{TOMATO} E13.5 embryos. (A) Overview of jugular and nodose ganglia. (B) Arrow heads show placode-derived *Phox2b*$^{TOM+}$ nodose neurons. Scale bar = 100µm

Taken together, in the current study, we analysed the development of cardiac innervation in functional connection with the morphogenesis of the heart and made following novel discoveries and observations. The first innervation of the cardiac primordium reaches the vicinity of the heart by E10.5 in mice. These nerves further deliver the precursors of the cardiac parasympathetic ganglia, SCPs, to the heart. Furthermore, we observed the cholinergic phenotype of the preganglionic nerves innervating the cardiac ganglia as well as of the neurons forming the paraganglia, as early as E13.5. This might mean that there might be a yet to be discovered role of acetylcholine during the early development of the cardiac nervous system, which possibly affects cardiogenesis itself. Furthermore, the vagal branch innervating the heart is comprised of mixed axons. Next to CHAT^{+} axons we also detect CHAT^{-} axons, which either express a different neurotransmitter or are still immature and do not possess any neurotransmitter phenotype yet. This again poses the question of the nature and role of

other early neurotransmitters released by embryonic nerves. Further, to assess the role of preganglionic spinal motor neurons in cardiac development, we analysed the formation of the cardiac ganglia as well as the cardiac morphology in the genetic *Hb9*$^{Cre/+}$;*Isl2*$^{DTA/+}$ strain. Development of the cardiac paraganglia is unaffected by the ablation of visceral motor neurons from the spinal cord. However, the cardiac structures, in particular the ventricular myocardium, exhibits morphological changes in this mutant strain. The exact cause of this phenotype however remains to be examined, since the ablation of the spinal motor neurons also causes a decrease in systemically circulating catecholamines. Nevertheless, this study reveals that the correct cardiac development is highly sensitive to external changes in the autonomic nervous system. Lastly, to lay down the basis for the thorough investigation of the exact mapping of cardiac innervation, we tested the validity of several specific markers to identify distinct neuronal subpopulations of the vagus nerve.

Discussion

In this study, my main question was how the embryonic cardiogenesis is influenced by the autonomic nervous system (ANS). More specifically, I was interested to reveal the significance and role of preganglionic sympathetic neurons in cardiogenesis and uncover possible changes in the developing heart due to the ablation of preganglionic sympathetic innervation. Many studies have been focusing on the neuronal control of the adult heart by the sympathetic and parasympathetic division of the ANS, but little is known about the neuronal contribution during cardiogenesis. In the last two decades many investigations targeting the interaction of the ANS and embryonic organogenesis revealed that the correct innervation plays a significant role in the development of several visceral organs (Furlan et al. 2017; Glebova and Ginty 2004; Kastriti et al. 2019; Knox et al. 2010; Nedvetsky et al. 2014). Knowing that peripheral nerves often support the correct establishment and maturation of visceral organs, I was curious to see whether preganglionic sympathetic neurons are crucial for the normal development of the murine heart. With the progression of this pursue, I discovered we are yet to describe in detail the temporal establishment of the cardiac nervous system. This led me to extend my aim to construct a thorough foundation explaining the molecular and cellular mechanisms underlying the interaction of the ANS and cardiogenesis. To achieve this aim, I, with the help of the Adameyko lab, performed a complex investigation with a variety of different experimental approaches covering the following aspects. First, to lay down the groundwork of this study, I investigated the cardiac innervation during embryonic development in wild type mice. Additionally, I studied the neurotransmitter profile of the preganglionic cardiac nerves and cardiac ganglia neurons. Next, I verified the usability of several markers, previously described to be specifically expressed in adult vagal sensory neurons, to identify sensory vagal subtypes innervating the embryonic heart. Lastly, to evaluate the importance of preganglionic sympathetic motor neurons, I analysed the genetic strain *Hb9*$^{Cre/+}$;*Isl2*$^{DTA/+}$, where I could efficiently eliminate visceral motor axons. In this model, *Hb9*$^{+}$ spinal motor neurons start expressing *Isl2*-driven DTA (Diphteria Toxin subunit A) upon exiting the cell cycle, leading to apoptosis of these cells.

I particularly focused on the formation of the cardiac ganglia as well as the structural development of the myocardium. Starting with the temporal establishment of normal cardiac innervation, my results obtained from immunostaining against NF200 in whole embryos and on cryosections of C57BL/6J mice, clearly demonstrate, that preganglionic axons arrive at the vicinity of the developing heart as early as E10.5 (Figure 1A, B). Only one other study so far investigated cardiac innervation at such early developmental stages (Hildreth et al. 2008). The focus of this previous study lies on deciphering the contribution of neural crest cells (NCCs) to the cardiac plexus (neuronal network, which comprises preganglionic cardiac innervation and paraganglia). With the utilization of the *Wnt1-Cre*;*R26R*^{lacZ} mouse line (Danielian et al. 1998; Soriano 1999; Epstein et al. 1991), they genetically traced NCC and its derivatives present in the cardiac primordium. *Wnt1* expression is initiated at early developmental stages (E9.0) in the neural plate throughout the presumptive neuroepithelium that will give rise to the midbrain and neural tube. Upon closure of the neural tube, *Wnt1* expression is restricted to distinctive regions, including also the dorsal midline of the neural tube, which is the origin of the neural crest (Echelard et al.1994; Wilkinson et al. 1987). In the *Wnt1-Cre*;*R26R*^{lacZ} mouse line, cells derived from the NC permanently express β-galactosidase (β-gal) and can be stained blue following a reaction with X-gal (Jiang et al. 2000). This frequently used method relies on the Cre-loxP system, in which expression of Cre-recombinase in NCCs or their derivatives genetically enables the expression of a Cre-reporter allele, thus permanently marking all neural crest-derived cells (Debbache et al. 2018). Without any further labelling, a differentiation between NC-derived subtypes of progeny populations is not possible. With this tracing, Hildreth and her team showed that neuronal cells derived from the NC (referring to cell which are double positive for and the neurofilament marker NF160D) are present in close proximity to the cardiac primordium at E12.5 (Hildreth et al. 2008). However, recent studies reveal, that these NC-derived cells, are in fact SCPs. Whole mount immunofluorescence staining against SOX10, a NC-specific TF essential for differentiation and maturation of SCP towards myelinating Schwann cells (Britsch et al. 2001; Kuhlbrodt et al. 1998), and neurofilament (NF) confirmed that by E11.5 all SOX10^{+} cells are associated with axons (or SOX10^{+};MITF^{+} melanoblasts). Therefore NCC free migration has ceased and SOX10^{+} cells settle on the nerves, hence changing into SCPs (Dyachuk et al. 2014). Furthermore, inducible genetic

tracing of SCPs in *Sox10::Cre*$^{ERT2/+}$*;R26R*$^{YFP/+}$ mice showed that approximately 70% of neurons in the parasympathetic cardiac ganglia are YFP^{+} cells when the animals were injected with tamoxifen (TAM) at E10.5. Recombination and start of tracing is induced with a delay since the injected tamoxifen has to be delivered to the liver and metabolised into its active form 4-hydroxytomoxifen (Donocoff et al. 2020; Nakamura et al. 2006). This proves that cardiac ganglia neurons derive from SCPs, which differentiate into autonomic neurons starting from E11.5. When the animals were injected at a later stage, such as E15.5, almost no YFP^{+} cardiac ganglia neurons could be detected (Dyachuk et al. 2014). Next to the TF *Sox10*, SCPs also transiently express *Phox2b* (Dyachuk et al. 2014; Espinosa-Medina et al. 2014), which is a key player in the development of sympathetic and parasympathetic neurons (Pattyn et al. 1999). In closer proximity to the developing organ, SCPs switch off the expression of *Phox2b* in order to differentiate into myelinating Schwann cells, whereas SCPs determined to become of neuronal nature acquire a SOX10^{-}/PHOX2B^{+} phenotype (Dyachuk et al. 2014; Espinosa-Medina et al. 2014; Kim et al. 2003; Nitzan et al. 2013). According to their location, these precursors can either give rise to adrenergic neurons of the sympathetic chain (Kastriti et al. 2019; Pattyn et al. 1999), or cholinergic neurons and glial cells of parasympathetic ganglia, including cardiac paraganglia (Dyachuk et al. 2014).

In the present study, I show for the first time, the early (E10.5) presence of nerve-associated SOX10^{+}/PHOX2B^{+} SCPs as well as detached cells that switched off the expression of either *Sox10* or *Phox2b* at the site of future cardiac ganglia. This brings final confirmation that the cardiac ganglia precursor cells are delivered by preganglionic nerves to the vicinity of the heart as early as E10.5 in mice.

With the discovery of SCPs being the precursors of autonomic ganglia, it also became evident that the formation of peripheral ganglia is dependent on the correct axonal establishment, as SCPs depend on the navigation to the primordia through peripheral nerves (Dyachuk et al. 2014; Espinosa-Medina et al. 2014). In *Pgk::Cre; Phox2a*^{ASIC2a} embryos, precursors of viscerosensory neurons are ablated in the epibrachial placode and, according to the expression schedule of *Phox2a* (Pattyn et al. 1997), visceromotor neurons undergo apoptosis upon exiting the cell cycle, resulting in complete absence of vagal axons. As expected, cardiac ganglia fail to form in these mutant embryos (Espinosa-Medina et al. 2014). The identity of the preganglionic axons innervating the

cardiac primordium detected by us cannot be clearly determined with the applied methods. However, by combining the information obtained from our whole mount data with immunofluorescence staining on cryosections (see figure 1), we conclude that they are most certainly branches of the vagus nerve. Furthermore, sympathetic postganglionic innervation develops and matures mainly shortly before birth and postnatally (Lipp and Rudolph 1972; Shigenobu et al.1988). These observations led us to exclude the sympathetic chain ganglia to be the source of the detected axons. Next, NC-derived cells differentiating into prospective neurons of the sympathetic chain are still mitotically active at E11.5, thus have not differentiated into mature sympathetic neurons and axonal outgrow is not initiated (Gonsalvez et al. 2013). To my best knowledge, no study has shown the temporal establishment and axonal outgrowth of sympathetic chain neurons to the heart. Therefore, to gain full assurance about the identity of the detected axons in this study, additional experiments have to be conducted. To trace the entire neuronal connection from the central nervous system down to the heart, I propose the utilization of a lipophilic stain such as 1,1´-dioctadecyl-3,3,3´,3´ tetramethylindocarbocyanine methanesulfonate (DiI). DiI is a fluorescent dye that diffuses laterally to stain the entire cell, which makes this method particularly useful to perform anterograde and retrograde tracing of entire neurons (Von Bartheld et al. 1990). DiI injection into the dorsal motor nucleus of the vagus (DMV) (Laughton and Powley 1987) and *nucleus ambiguus* (NA) (Ai et al. 2007) in the brainstem traces parasympathetic motor neurons (MNs), whereas injection into the vagal sensory ganglia (nodose and jugular ganglion) labels viscerosensory neurons of the vagus nerve (Kupari et al. 2019). Injection into either of the sensory ganglia however is accompanied with possible co-labelling of vagal MNs, since vagal efferent axons bypass these structures. Another option is the injection into the cardiac primordium, which would allow for retrograde tracing of the innervating axons back to their origin. Modifications of existing lipophilic dyes led to the introduction of DiI-analogues such as CM-DiI, SP-DiI and FM 1–43FX, which possess both the property of adhering to the cellular membranes and protein structures. These analogues allow to application of subsequent tissue clearing methods, since the modified properties remedy the wash-out of the lipophilic dye by clearing agents, which are relying on the removal of lipids (Jensen and Berg 2016). Combining the application of such DiI-analogues with subsequent immunostaining

against markers for potential neurotransmitters, such as acetylcholine and norepinephrine, and clearing methods in the developing mouse embryo would reveal the temporal, spatial and molecular development of the peripheral nerves innervating the heart. Next to the application of lipophilic dies, viral neuronal tracing is another well-established method. Adeno-associated virus (AAV), a single-strand DNA virus, is commonly used for *in vivo* gene transfer since it is not associated with disease in humans and has been shown successful to induce stable long-term expression of transgenes in a plethora of tissues. Additionally, the motifs on the capsid surface, which are critical for the attachment to the host cells, can be modified resulting in cell specific targeting of the vector (Chan et al. 2017; Van Vliet et al. 2008). One specific capsid variant, AAV-PHP.S, has been shown to specifically transduce peripheral neurons, including cardiac ganglia neurons (Chan et al. 2017; Rajendran et al. 2019). Genetic tracing and classic immunohistochemical approaches using selective markers for motor and sensory neurons, are also applicable to discriminatively label the two compartments of the vagus nerve with the goal to identify the nature and development of the cardiac innervation. For example, *Vglut2* and *Chat* are largely selective markers for sensory and motor neurons of the vagus nerve (Chang et al. 2015). To demarcate the different vagal sensory subtypes, ganglia specific markers have to be employed. Here, we validated the applicability of the previously described makers *Phox2b* and *Prdm12,* to discriminately label embryonic nodose and jugular neurons of the vagal nerve (Dauger et al. 2003; Desiderio et al. 2019; Kupari et al. 2019; Marmigère and Ernfors 2007). This was an effort to determine a way for embryonic studies of these two subgroups of vagal neurons since most studies investigating sensory neurons of the nodose and jugular ganglia are conducted in adult animals (Berthoud and Neuhuber 2000). We show that at E13.5 the gene *Phox2b* is selectively expressed in placode derived nodose ganglion neurons, whereas *Prdm12* is solely expressed in neurons originating in the NC-derived neurons of the jugular ganglion (Kupari et al. 2019; Nassenstein et al. 2010). These results allow for the utilization of these genes to employ genetic tracing or ablation of these specific sensory subtypes during development. However, both genes are further essential for the development of other neuronal cell types and widely expressed in several cell populations. Neurons of the trigeminal ganglion (TG) and dorsal root ganglia (DRG) are expressing *Prdm12* (Desiderio et al. 2019).

Phox2b is a crucial transcription factor for all autonomic neural crest derivatives, including cranial and spinal motor neurons originating in the brain stem and spinal cord, respectively, as well as for placode-derived viscerosensory neurons. A genetic knock out of *Phox2b* leads to a complete loss of all autonomic neural crest derivatives, which includes the superior cervical ganglion, the sympathetic chain and the enteric nervous system, additionally to the absence of the three epibranchial placode-derived visceral sensory ganglia of the VIIth, IXth and Xth cranial nerves (Pattyn et al. 1997, 1999). Therefore, the identification and validation of additional genes more specific to vagal sensory neuronal subtypes is pivotal for distinctly targeting these neurons. Some studies indicate that vagal sensory control of cardiac functions seems to be solely conducted by nodose ganglion neurons (Chang et al. 2015; Kupari et al. 2019; Marmigère and Ernfors 2007); there is no evidence so far for the presence of afferent jugular neurons innervating the heart. Two potential candidates to discriminate between nodose afferent subtypes are the genes *P2ry1* and *Npy2r* (Chang et al. 2015; Kupari et al. 2019). Viscerosensory neurons expressing either of these genes are found to innervate the heart. Activity of *Npy2r* expressing afferents was shown to decrease the heart rate, while the effect of *P2ry1* neurons on cardiac function remains unclear (Chang et al. 2015).

Next to sensory innervation, the heart receives neuronal input of vagal efferent axons originating in the *nucleus ambiguus* (NA) and the dorsal motor nucleus of the vagus nerve (DmnX), exhibiting differential control over postganglionic cardiac neurons (Ai et al. 2007; Bieger and Hopkins 1987; Cheng et al. 2004; Cheng and Powley 2000; McLean and Hopkins 1982). However, most of these studies are conducted in adult animals and little is known about the embryonic role of parasympathetic cardiac innervation. We therefore wanted to address the presence and role of embryonically released neurotransmitter by preganglionic parasympathetic neurons innervating the developing heart. The neurotransmitter phenotype of adult parasympathetic neurons is well studied. However, during embryogenesis some neurons often exhibit a transient phenotype or do not release any neurotransmitter until very late in development (Apostolova and Dechant 2009). We therefore aimed to elucidate the question of functional roles of this early innervation in light of signalling molecules released by these axons. Naturally, we first investigated the presence of the main neurotransmitter of

parasympathetic neurons, acetylcholine (ACh), in the embryonic vagus nerve. Using the expression of the gene coding for choline acetyltransferase (*Chat*), a transferase enzyme responsible for the synthesis of ACh, we genetically trace cholinergic neurons with the *Chat-Cre;R26R*^{TOMATO} mouse strain. We show that preganglionic axons (presumably of the vagus nerve; nX) innervating the cardiac paraganglia already exhibit a cholinergic phenotype at E13.5 (nX in figure 2B, 2C). Furthermore, neurons of the cardiac paraganglia also start expressing *Chat* by this stage (PHOX2B^{+}/*Chat*$^{TOM+}$ cells; arrowheads in figure 2C). Fregoso and Hoover showed that by E18.5 (no analysis of earlier stages) some cardiac ganglia neurons are immunoreactive for vesicular acetylcholine transporter (VAChT), indicating as well that cardiac ganglia form and develop a cholinergic phenotype already prenatally (Fregoso and Hoover 2012). We therefore propose the hypothesis of acetylcholine and possibly other neurotransmitters possessing yet to be discovered signalling roles during cardiac development, including both cardiogenesis itself and the maturation the cardiac nervous system. As described earlier, some tissues are dependent on nerve innervation during organogenesis; one example is the crucial cholinergic input from parasympathetic nerves to the submandibular gland for its correct development (Knox et al. 2010). Consequently, acetylcholine might also play a morphogenetic role in the correct formation of the embryonic heart. Further, we also see CHAT^{-} axons contributing to the innervating nerve, which presumably belong to immature neurons that either use another neurotransmitter or do not express any neurotransmitter yet. Next to ACh, some parasympathetic neurons also contain non-cholinergic neurotransmitters and neuromodulators such as nitric oxide (NO) (Paton, Kasparov, and Paterson 2002) and vasoactive intestinal peptide (VIP) (Henning and Sawmiller 2001). The physiological role of NO in the cardiac nervous system in mice is not entirely clear yet. However, in other species (rat), networks of intracardiac parasympathetic neurons are thought to play an essential role in the integration of signals from the vagal efferent and local sensory fibres (Pauza et al. 1997; Rysevaite et al. 2011). NO is a recognized modulator of synaptic plasticity in the CNS and PNS (Förstermann and Sessa 2012; Shefa et al. 2018) and also known to influences the excitability of cardiomyocytes, regulate the heart rate as well as intrinsic cardiac neuronal activity (Armour et al. 1995; Altememi and Alkadhi 1999; Hogan et al. 1999; Paton et al. 2002). It is therefore highly integrated in the autonomic

control of cardiovascular function and contributes to the dysfunction of the parasympathetic and sympathetic nervous system in many cardiovascular diseases (Zucker et al. 2004). Nevertheless, all studies concerning the role of NO in the cardiac nervous system are focusing on functional aspects and are conducted in adult animals and only very little is known about the contribution of NO and other neuromodulators during cardiac development. The role of signalling cues from non-classical neurotransmitters, such as NO, on cardiac development might therefor be yet another part to be unravelled. To recap, we show that both preganglionic axons and cardiac paraganglia neurons exhibit a cholinergic phenotype already at E13.5. Further, we also see $CHAT^-$ axons contributing to the innervating nerve, which presumably belong to immature neurons that either use another neurotransmitter or do not express any neurotransmitter yet. Relating our findings with the recent discoveries, describing the necessity of the ANS for the normal development of several visceral organs (Borden et al. 2013; Furlan et al. 2017; Glebova and Ginty 2004; Knox et al. 2010; Soldatov et al. 2019), it becomes evident that there are still to be discovered possible contributions of cardiac innervation supporting and governing cardiogenesis. I propose a series of experiments to investigate the role of molecules released by embryonic preganglionic axons, to elucidate the network of signalling cues connecting the peripheral nervous system and the correct development, maturation and function of the murine heart. Many studies in the adult mammalian heart have shown the presence of muscarinic and nicotinic acetylcholine receptors in ventricular and atrial cardiomyocytes (Bibevski et al. 2000; Yang et al. 2005; van Zwieten and Doods 1995). In contrast, there is only limited data as well as discrepancies in the literature as to the presence and functionality of acetylcholine receptors in cardiomyocytes during early embryonic stages (Dvorakova et al. 2005; Nedoma et al.1986; Nenasheva et al. 2013). One study shows cholinergic receptor response at E10.5 in the mouse heart (Chen, Klitzner, and Weiss 2006), however another reports response to acetylcholine only after E13 with a steady increase until birth (Wildenthal 1973). Regarding the detection of nicotinic receptors in the fetal heart, there have been no studies so far. According to Eurexpress (see link under "References" – CHRNA4 Eurexpress), nicotinic acetylcholine receptor alpha 4 (CHRNA4) is present in ventricular myocardium at E14.5, but when looking for expression of *Chrna4* (mRNA) (see link under "References" – *Chrna4* Allen Brain Atlas), there is no

detectable signal. Immunofluorescence staining against the muscarinic and nicotinic receptors can readily verify the presence or absence of these receptors. Additionally, pharmacological treatment by administration of antagonists of the muscarinic (e.g. atropine) and the nicotinic (e.g. mecamylamine) receptor types could further aid understand the role of cholinergic signalling in cardiac development. The utilization of genetic models to ablate the cholinergic phenotype, such as Chat KO, and subsequent analysis of the developing heart would be another approach to analyse the function of ACh in cardiogenesis. The combination of these approaches with morphological analyses of the heart via volumetric imaging methods such as whole embryo immunofluorescent stainings or computer tomography (microCT) scanning could reveal more details about the effects of these signalling cues on the cellular proliferation, differentiation and orientation of cardiomyocytes.

In addition to parasympathetic innervation, the heart further receives neuronal input from sympathetic neurons of the middle cervical and stellate ganglion of the sympathetic chain (Pardini, Lund, and Schmid 1989). The sympathetic chain is innervated by preganglionic motor neurons from the spinal cord. To investigate the role of spinal control on the heart via the sympathetic chain ganglion (SCG), we specifically ablated preganglionic motor neurons. For this we utilized the *Hb9*$^{Cre/+}$; *Isl2*$^{DTA/+}$ strain (Yang et al. 2001), which has been previously used to investigate the role of preganglionic neurons as the delivery route for precursor cells (SCP) to target organs such as the adrenal gland (Furlan et al. 2017) and the ZO organ (Kastriti et al. 2019). First, we examined the sympathetic chain ganglia (SCG) at levels from the aortic arch to the more rostral located adrenal gland and Zuckerkandl organ. We observe that neurons of the SCG are not affected by the loss of preganglionic motor neurons (figure 3D). Since the sympathetic neurons of the paravertebral chain are NC-derived, the formation of the SCG does not depend on preganglionic nerves for migration of precursor cells (Le Douarin and Kalcheim 2011; Etchevers et al. 2019). Nevertheless, observing no phenotype in the SCG neurons, led us to the conclusion that the preganglionic motor neurons most likely do not provide indispensable trophic support for sympathetic postganglionic neurons. Another explanation for the undisrupted development of the SCG could be the model in question spares some of the traversing viscerosensory axons connecting the spinal cord and the SCG. Next, we focused on the formation of the cardiac ganglia. We detect

normally developed paraganglia, leading to the conclusion that the cardiac ganglia form normally in the absence of trophic support of the spinal motor neurons. Even though this is not too surprising, it could still have been possible to detect some malformations due to a disrupted connection between spinal visceral motor neurons and the cardiac ganglia which has not been detected yet.

In contrast to this, analysis of the adrenal medulla shows a significant alteration in these mutant embryos, which was to be expected. By ablation of preganglionic MNs, the delivery route of the precursor (SCPs) of the endocrine neurons to one of the major chromaffin organs in mammals, the adrenal medulla, is disrupted. Consequently, *Hb9*$^{Cre/+}$; *Isl2*$^{DTA/+}$ mutant embryos exhibit a significant decrease in circulating catecholamines (Furlan et al. 2017; Kastriti et al. 2019). Catecholamines play not only a central role in stress-response in the adult organism, but are also fundamental during embryonic development, including normal cardiac development (Portbury et al. 2003). Several studies showed that norepinephrine (NE) in particular, but also epinephrine and dopamine, are essential for fetal mouse development, since knockout mice lacking catecholamines, specifically NE, became necrotic at E12.5 (Pattyn et al. 1999; Thomas et al. 1995; Zhou et al. 1995). Foetuses lacking NE display a high heterogeneity in structural abnormalities of cardiomyocytes, the cells appear disorganized and atrophied (Thomas et al. 1995). However, this is the only study so far investigating the effect of lacking NE on the cardiac structural development. Furthermore, this study does not clarify whether the cardiac phenotype is caused by a direct or secondary effect of the missing catecholamines. Other studies showed a disturbed physiology of the heart due to the lack of catecholamines (Thomas et al. 1995). Tyrosine hydroxylase deficient (*TH*$^{-/-}$) foetuses lack catecholamines and some show symptoms of congestive heart failure at E12.5 (Zhou et al. 1995). As *Phox2b* is the central regulator for the correct establishment of the vertebrate noradrenergic phenotype, expression of *Th* and *Dbh* (dopamine hydroxylase) is absent in *Phox2b*$^{LacZ/LacZ}$ animals. *Phox2b*-null embryos die midgestation (E12.5), however lethality could be rescued by exogenous administration of NE to the mother (Pattyn, Goridis, and Brunet 2000). In contrast, mice lacking only epinephrine are fully viable (Zhou et al. 1995). Even though it has been established that the adrenergic system plays a critical role in ontogeny, the exact mechanism of catecholamines influencing proliferation and differentiation of cardiac progenitors and cardiomyocytes

in the embryonic heart still need to be unravelled. There is evidence suggesting that β-adrenergic receptor responses in the embryonic heart develop at E9.5, whereas the first sympathetic neurons innervating the heart were only detected by E14.5 (Chen et al. 2006) and embryonic neuroendocrine chromaffin cells (catecholamine expressing) are not in place before E13.5 (Furlan et al. 2017; Kastriti et al. 2019), therefore NE from the mother might act in a paracrine manner.

Thus, to evaluate the significance of the decrease of catecholamines, and the absence of visceral motor neurons, in the cardiac development, we performed additional analyses of the cardiac morphology. Either of these phenotypes could cause possible malformations in the embryonic heart. To obtain accurate three-dimensional images of the heart and its surrounding structures we employed x-ray microtomography (microCT). With correct contrast staining it is nowadays possible to visualize non-mineralized tissues, such as the soft tissues of organs (Metscher 2009). Whole embryo immunofluorescent staining is another commonly used method for volumetric imaging. However, due to the late developmental stage (E18.5) we chose to analyse, this method was not suitable. We observe that the volume of the total ventricular myocardium is reduced in the mutant *Hb9*$^{Cre/+}$;*Isl2*$^{DTA/+}$ hearts. Also, by normalizing the volume of the interventricular septum (IVS) to the total ventricular volume, we see possible hypotrophy of the IVS. Additionally the asymmetry between the left and right ventricle (LV > RV) seems to be less distinct in *Hb9*$^{Cre/+}$;*Isl2*$^{DTA/+}$ embryos. A clear statement is however difficult, since we also detect some mutant and control hearts with a smaller LV than RV. An explanation for this could be that during fetal blood circulation only a small percentage of total cardiac output is directed towards the lung. This results in a limited pulmonary venous input into the left ventricle, which itself leads to a dominant right ventricle in the embryo (Rudolph 1985). Another possible reason for our observation could be variations in the measurements. We obtained the volumes of ventricles by segmenting the inner cavity of the LV and RV. The microCT images clearly show the cardiac structures, since the contrast between stained muscle cells and air is very high. Nevertheless, in case of residual blood, which has roughly the same contrast as muscle cells, distinction between ventricular myocardium and blood is very difficult to impossible. In these cases, segmentation was based on estimations. This could have led to distorted measurement of the actual volumes. Another observation in the

Hb9$^{Cre/+}$;*Isl2*$^{DTA/+}$ hearts regards the atrial morphology. As visible in the 3D volume rendering (figure 4E), the atrial appendages of some *Hb9*$^{Cre/+}$;*Isl2*$^{DTA/+}$ hearts exhibit abnormal formation or appear smaller in size, compared to *Isl2*$^{DTA/+}$ hearts. However, during the cardiac cycle, which includes ventricular and atrial systole (contraction) and diastole (relaxation), the atrial appendages also undergoes structural changes (Katz 2011). We only focused on the ventricular conformation and categorized the samples into contracted and relaxed ventricular state, which is slightly asynchronous with the atrial systole/diastole cycle. Atrial systole occurs at the end of ventricular diastole, while atrial diastole overlaps with both ventricular systole and diastole (Katz 2011). A separation into ventricular contraction and relaxation therefore does not account for a distinct identification of the atrial state, which would be crucial for atrial volumetric comparison between the mutant *Hb9*$^{Cre/+}$;*Isl2*$^{DTA/+}$ and control *Isl2*$^{DTA/+}$ hearts. Finding methodological ways to stop the heartbeat in a distinct state would remedy these obstacles, but to our knowledge there is no way to achieve this reproducibly to date.

All of the described manifestations in the mutant *Hb9*$^{Cre/+}$;*Isl2*$^{DTA/+}$ hearts bring us to the conclusion that the ablation of spinal motor neurons and furthermore a systemic decrease of circulating catecholamines, has an effect on the cardiac and in particular the ventricular development. Nevertheless, additional investigations have to be conducted in order to fully understanding of the causes and effects leading to this phenotype. At this point in time, the low power of statistical analysis requires many more hearts from both the control and experimental conditions to establish the presence or absence of formal statistical significance. This word will be continued. Furthermore, in the near future we are planning to perform the same analysis using a second genetic model, *Olig2*^{Cre};*Rosa26*^{lxstopDT} (Wang et al. 2014), which exhibits a similar phenotype due to a complete ablation of spinal motor neurons. This is an attempt to reproduce our results described here, to further support our claimed hypothesis. Besides the cardiac phenotype caused by the mutation, we also observe a great variation within the same cardiac state and genotype regarding the relative size of the ventricles and the atria. This naturally occurring developmental variation was to be expected, especially since embryonic mouse development is asynchronous within the same litter. This variation could potentially mask the differences between the genotypes. Again, a greater sample size could potentially compensate for this naturally occurring variation and allow for a

significant and detailed statement about the cardiac phenotype in the *Hb9*$^{Cre/+}$;*Isl2*$^{DTA/+}$ strain. Additional investigation of the normal cardiac development during embryonic stages E14 to E18 could help for better judgment of variance in size and morphology of the developing mammalian heart. Furthermore, a physiological defect of the *Hb9*$^{Cre/+}$;*Isl2*$^{DTA/+}$ heart cannot be excluded. Embryos die shortly after birth due to missing sympathetic innervation of the lungs (data not shown). In utero investigations monitoring the heart rate would possibly bring additional insights to the cardiac changes in this mutant strain. Lastly, the absence of circulating norepinephrine and epinephrine, which both are essential during embryogenesis, in mutant *Hb9*$^{Cre/+}$;*Isl2*$^{DTA/+}$ embryos could potentially be compensated by maternal catecholamines transferred via the placenta. Bringing back the role of cardiac innervation into the equation, I moreover propose the utilization of the genetic models *Ascl1*^{CreERT2} KI and *Sox10*^{CreERT2};*R26R*^{DTA} to specifically ablate the intrinsic cardiac innervation (parasympathetic cardiac ganglia) and sympathetic ganglia (stellate ganglion) by inducing cell death of the NCCs and SCPs respectively that normally will give rise to the ganglia.

To conclude, this thesis contributes several new insights to the closely regulated and highly intertwined connections of the peripheral nervous system and the embryonic development of the mammalian heart. Moreover, I disclose that there are still wide gaps of knowledge regarding the neuronal contributions in early cardiogenesis despite the decades of comprehensive research in the field of embryology and organogenesis, which clearly supports the importance of further studies. Last but not least, the current project unveiled an additional interplay between peripheral nerves and orchestration of the development of inner organs (in this case the heart), which can fuel a plethora of future projects.

Methods and Material

Mouse strains

For all experiments, male and female mice were mated overnight to generate timed pregnancies; the day the plug was detected was considered as E0.5 and the day the mice were born was considered as postnatal day 0 (P0).

Hb9-Cre mice were received from The Jackson Laboratory (stock 006600). *Isl2*^{DTA} mice were received from The Jackson Laboratory (stock 007942). *Chat-Cre* mice were received from K. Meletis lab (Karolinska Institutet); also available from the Jackson Laboratory, stock number 006410 (full strain name B6;129S6-Chattm2(cre)Lowl/J). *Phox2b-Cre;R26R*^{TOMATO} mice were received from the Jean-François Brunet laboratory (D'Autréaux et al. 2011).

Motor neuron ablation experiments

For targeted ablation of the preganglionic neurons, *Isl2*^{DTA} mice were bred to *Hb9-Cre* mice to generate experimental *Hb9*$^{Cre/+}$;*Isl2*$^{DTA/+}$ and control *Isl2*$^{DTA/+}$ embryos. *Isl2*$^{DTA/+}$ n=5; *Hb9*$^{Cre/+}$;*Isl2*$^{DTA/+}$ n=8.

Embryo preparation for cryosections

After sacrificing the pregnant mouse, the uterus containing the embryos was removed and placed in a petri dish filled with 1x phosphate-buffered saline (PBS) on ice. The embryos were eviscerated one by one and placed in fresh PBS and washed twice for 10 min. For embryos older than E14.5, a small incision was made in the anterior abdominal wall and the neck for better solution penetration. The embryos were fixed in 4% (w/v) paraformaldehyde (PFA) at 4°C with rotation for the following durations: E10.5 - E11.5 for 3 to 3.5 hrs, E12.5 - E13.5 for 4 to 4.5 hrs, E14.5 - E15.4 for 5 to 6 hrs, E16.5 and older overnight (12 - 18 hrs).

Immunohistochemical staining

Tissue samples were embedded in OCT (optimal cutting temperature compound) and frozen at −20°C. Frozen tissue was sectioned (cryosections) on the cross-sectional or sagittal plane at 14–18 µm and frozen at −20°C after drying at room temperature (RT)

for at least 1 h. Antigen retrieval was performed by incubating the sections in 1x Target Retrieval Solution (Dako, S1699) for 40 min, pre-heated at 80°C and cooled down to RT. Sections were washed three times in PBST (phosphate-buffered saline with 0.1% Tween^{TM} 20), 5 min each time, and incubated at 4°C overnight with primary antibodies diluted in PBST. Finally, sections were washed three times in PBST, 5 min each, and incubated with secondary antibodies diluted in PBST at room temperature for 1 h, washed three times in PBST and mounted using Mowiöl mounting medium. When DAPI (binds strongly to adenine–thymine-rich regions in DNA and therefore labels the cell body) was used, it was diluted in PBST to a concentration of 0.1mg/mL and added to the samples together with the secondary antibodies. All primary antibodies and the used concentrations are listed in the table below. For detection of the primary antibodies, we used the following secondary antibodies. Anti-mouse, anti-rabbit, anti-goat and anti-guinea pig raised in donkey and conjugated with Alexa-488, -555, 647 fluorophores in the concentration 1:1000 from Molecular Probes, Thermo Fisher Scientific. Anti-chicken raised in donkey conjugated with Alexa-488 and -647 or with Cy3 fluorophores in the concentration 1:600 from Jackson ImmunoResearch.

Table 1. Primary antibodies used for immunofluorescence on cryosections and in whole embryos.

Description	Species	Clone	Company	Catalog #	Concentration*
anti-ISL1	rabbit	polyclonal	SySy	406 003	1:1000
anti-ISL1	mouse	monoclonal	DSHB	39.4D5	1:250
anti-PGP9.5	rabbit	polyclonal	Novus Biologicals	NB300-675	1:750
anti-PHOX2B	rabbit	polyclonal	Pattyn et al. 1997	n.-c.	1:500
anti-PHOX2B	goat	polyclonal	R&D Systems	AF4940	1:500
anti-SMA	mouse	monoclonal	Sigma Aldrich	A5228	1:500 (1:1000)
anti-SOX10	mouse	monoclonal	Santa Cruz	sc-365692	1:50
anti-SOX10	goat	polyclonal	Santa Cruz	17342	1:500 (1:500)
anti-TH	rabbit	polyclonal	Pel-Freeze Biol.	P40101-150	1:1000
anti-TH	guinea pig	polyclonal	SySy	213 104	1:500
anti-TH	mouse	monoclonal	Sigma Aldrich	T2928	1:1000
anti-NF200	chicken	polyclonal	Abcam	ab4680	1:1000 (1:1000)
anti-NF-M	mouse	monoclonal	DSHB	2H3	1:100
anti-mCherry	chicken	polyclonal	EnCor Biotech	CPCA-mCherry	1:1000

*Used concentration is given for cryosections or whole mount (WM; in brackets). n.-c., non-commercial

Whole mount *in situ* hybridization chain reaction

The following procedures were performed at room temperature if not stated otherwise. After fixation in 4% PFA for 5 or 20 hours (two different approaches; overfixation recommended for HCR; normal fixation time of 4-5 hours for E13.5), samples were washed twice in PBST for 10 minutes. Following, the samples were dehydrated through a graded series of methanol / PBST (25% MeOH / 75% PBST, 50% MeOH / 50% PBST, 75% MeOH / 25% PBST, 100% MeOH) washes. Each wash was performed for 1 hour (for E13.5) at 4°C with rotation; the last wash (100% MeOH) was repeated twice to fully dehydrate the tissue. Subsequently the samples were put in fresh 100% methanol and stored overnight (at least 16 h) at -20°C. Before probe hybridization, the samples have to be rehydrated again. For this, the graded series of MeOH / PBST washes described above was reversed, starting with 75%MeOH / 25%PBST, ending with 100% PBST. Again, each step was performed at 4°C with rotation; the last wash (100% PBST) was repeated twice. Treatment with 20 µg/mL proteinase K solution for 30 minutes (for E13.5) facilitates

access to the target nucleic acid. Proteinase K concentration and treatment time should be adapted to the developmental stage of the samples. After this treatment the samples were washed twice in PBST for 5 min, postfixed with 4% PFA for 30 min and washed again with PBST three times for 5 min. For the further procedures, the samples were transferred to a 2 mL tube (1-4 embryos per tube). The following steps are presenting the so-called detection stage. The samples were incubated in 1mL of hybridization buffer for 5 min, subsequently the buffer was renewed, and the samples were pre-hybridized for 30 min at 37°C. Following the protocol, the probe solution was prepared by adding 2pmol of each probe mixture to 500 µL of probe hybridization buffer at 37°C. After removing the pre-hybridization buffer and adding the probe solution, the samples were incubated overnight (12-16 h) at 37°C. The excess probes were removed by washing the embryos four times for 15 min with 1 mL of probe wash butter at 37°C and twice with 5x saline-sodium citrate (SCC) buffer for 5 min. For the amplification stage, the embryos are pre-amplified with 1mL of amplification buffer for 5 min. The preparation of the hairpins was done by separately snap cooling 30 pmol (10 µL of 3 µM stock) of hairpin h1 and hairpin h2. For this, the hairpins h1 and h2 (in separate tubes) were heated up at 95°C for 90 seconds and cooled back down to room temperature in the dark (dark drawer) for 30 min. The hairpins were provided in hairpin storage buffer ready for snap cooling. The snap cooled hairpins h1 and h2 were added to 500 µL of amplification buffer. The pre-amplification buffer was removed, and the hairpin mixture was added to samples and incubated overnight in the dark. To remove the excess hairpins, the samples were washed with 1 mL of 5x SSC buffer, twice for 5 min, then twice for 30 min and again for 5 min. The samples were stored at 4°C and protected from light before microscopy.

For detection of nodose and jugular neurons we used probes against the genes *Phox2b* (NM_008888.3) and *Prdm12* (NM_001123362.1). All reagents are purchased from Molecular

Instruments, Inc.

Microscopy

For immunohistochemistry and HCR, images were acquired using LSM 880 Zeiss confocal microscope equipped with 10x and 20x objectives. Images were acquired in the .lsm format and processed with ImageJ (FIJI) (Schindelin et al. 2012). Projection of z-stacks

was always done with projection type “Max Intensity”. Images were exported as .tiff files for further processing in Adobe Photoshop CS and Adobe Illustrator.

MicroCT imaging

Sample preparation and contrast staining

In order to obtain full and even staining, we reduced the size of the sample by removing the lower body and the head (dissections above the thymus and below and abdominal wall). This allows for better dehydration and faster migration of the staining reagents. After fixation in 4% PFA, the samples were dehydrated in methanol. To prevent abrupt shrinkage a graded series of methanolic solutions was used. Beginning with 25% MeOH / ddH_2O followed by 50%, 75%, 90% MeOH, each washing step was done for 24 hours at 4°C with rotation. We used two of the most broadly used contrast stains for soft tissue, inorganic iodine (in 90% MeOH or EtOH) and phosphotungstic acid (PTA) (Metscher 2009). With the use of the contrast reagent PTA, to increase the intrinsically low X-ray absorption of non-mineralized tissue, we obtained high resolution microCT images of the developing heart. We stained with 1% PTA in 90% MeOH for 48hrs at room temperature with rotation. The staining time depends on the size, developmental stage and composition of the tissue of the sample. We found 48hrs to be sufficient to fully stain the upper trunk (lower trunk and head were removed) of E18.5 embryos. It has to be clarified however, such a short incubation time for this stage was only sufficient due to the reduction of the sample size and the two open (cut) surfaces of the samples. Other protocols employ drastically longer incubation times for this stage; however, these protocols refer to whole embryos and are often performed at 4°C.

Imaging settings of microCT scans

For scanning the samples were embedded in 1% low melting-temperature agarose in 5ml vials. Samples were imaged using XRadia MicroXCT system with a 5µm voxel resolution. All images were reconstructed using the provided software by XRadia MicroXCT and binned by 2 x 2 pixels to increase signal-to-noise ratio, as well as to reduce image file size. All reconstructed volumes were exported as images stacks in .tiff format.

Three-dimensional image analysis and segmentation

For segmentation and subsequent volumetric analysis, we used the 3D Visualization & Analysis Software Amira-Avizo (ThermoFisher^{TM}).

To allow a qualitative comparison of the cardiac structures in the mutant *Hb9*$^{Cre/+}$;*Isl2*$^{DTA/+}$ and control *Isl2*$^{DTA/+}$ embryos, we chose distinct cardiac landmarks in the sagittal, cross and transverse planes of the heart. The sagittal plane shows the interventricular septum (IVS) and the right atrium (RA) joining the right ventricle (RV), which has been virtually cut off in this view. Further, at this level the pulmonary trunk (PT) can be seen entering the right ventricle (RV) and the ascending aorta (Aao), which is bending contralateral towards the left ventricle (RA). The cross section has been chosen at approximately midlevel of the anterior and posterior pole of the IVS. The left and right ventricles can be seen from the posterior view. The transverse plane virtually cuts the heart across the level where the aortic trunk enters the LV. The left and right atria and ventricle, as well as the IVS can be seen at this plane.

References

Adameyko, Igor, Francois Lallemend, Jorge B. Aquino, Jorge A. Pereira, Piotr Topilko, Thomas Müller, Nicolas Fritz, Anna Beljajeva, Makoto Mochii, Isabel Liste, Dmitry Usoskin, Ueli Suter, Carmen Birchmeier, and Patrik Ernfors. 2009. "Schwann Cell Precursors from Nerve Innervation Are a Cellular Origin of Melanocytes in Skin." *Cell* 139(2):366–79.

Ai, J., P. N. Epstein, D. Gozal, B. Yang, R. Wurster, and Z. J. Cheng. 2007. "Morphology and Topography of Nucleus Ambiguus Projections to Cardiac Ganglia in Rats and Mice." *Neuroscience* 149(4):845–60.

Altememi, G. F. and K. A. Alkadhi. 1999. "Nitric Oxide Is Required for the Maintenance but Not Initiation of Ganglionic Long-Term Potentiation." *Neuroscience* 94(3):897–902.

Anderson, David J. 1999. "Lineages and Transcription Factors in the Specification of Vertebrate Primary Sensory Neurons." *Current Opinion in Neurobiology* 9(5):517–24.

Apostolova, Galina and Georg Dechant. 2009. "Development of Neurotransmitter Phenotypes in Sympathetic Neurons." *Autonomic Neuroscience: Basic and Clinical* 151(1):30–38.

Arber, Silvia, Barbara Han, Monica Mendelsohn, Michael Smith, Thomas M. Jessell, and Shanthini Sockanathan. 1999. "Requirement for the Homeobox Gene Hb9 in the Consolidation of Motor Neuron Identity." *Neuron* 23:659–74.

Armour, J. A., F. M. Smith, A. M. Losier, H. H. Ellenberger, and D. A. Hopkins. 1995. "Modulation of Intrinsic Cardiac Neuronal Activity by Nitric Oxide Donors Induces Cardiodynamic Changes." *American Journal of Physiology - Regulatory Integrative and Comparative Physiology* 268(2 37-2).

Asensio, Cédric, Maria Jimenez, Françoise Kühne, Françoise Rohner-Jeanrenaud, and Patrick Muzzin. 2005. "The Lack of β-Adrenoceptors Results in Enhanced Insulin Sensitivity in Mice Exhibiting Increased Adiposity and Glucose Intolerance." *Diabetes* 54(12):3490–95.

Von Bartheld, C. S., D. E. Cunningham, and E. W. Rubel. 1990. "Neuronal Tracing with DiI: Decalcification, Cryosectioning, and Photoconversion for Light and Electron Microscopic Analysis." *Journal of Histochemistry and Cytochemistry* 38(5):725–33.

Berthoud, Hans-Rudolf and Winfrid L. Neuhuber. 2000. "Functional and Chemical Anatomy of the Afferent Vagal System." *Autonomic Neuroscience: Basic and Clinical* 85(1–3):98–101.

Bibevski, Steve, Yuefang Zhou, J. Michael McIntosh, Richard E. Zigmond, and Mark E. Dunlap. 2000. "Functional Nicotinic Acetylcholine Receptors That Mediate Ganglionic Transmission in Cardiac Parasympathetic Neurons." *Journal of Neuroscience* 20(13):5076–82.

Bieger, Detlef and David A. Hopkins. 1987. "Viscerotopic Representation of the Upper Alimentary Tract in the Medulla Oblongata in the Rat: The Nucleus Ambiguus." *Journal of Comparative Neurology* 262(4):546–62.

Borden, Philip, Jessica Houtz, Steven D. Leach, and Rejji Kuruvilla. 2013. "Sympathetic Innervation during Development Is Necessary for Pancreatic Islet Architecture and Functional Maturation." *CellReports* 4(2):287–301.

Brand, Thomas. 2003. "Heart Development: Molecular Insights into Cardiac Specification and Early Morphogenesis." *Developmental Biology* 258(1):1–19.

Briscoe, James, Alessandra Pierani, Thomas M. Jessell, and Johan Ericson. 2000. "A Homeodomain Protein Code Specifies Progenitor Cell Identity and Neuronal Fate in the Ventral Neural Tube." *Cell* 101(4):435–45.

Britsch, Stefan, Derk E. Goerich, Dieter Riethmacher, Reto I. Peirano, Moritz Rossner, Klaus Armin Nave, Carmen Birchmeier, and Michael Wegner. 2001. "The Transcription Factor Sox10 Is a Key Regulator of Peripheral Glial Development." *Genes and Development* 15(1):66–78.

Carmeliet, Peter and Marc Tessier-Lavigne. 2005. "Common Mechanisms of Nerve and Blood Vessel Wiring." *Nature* 436(7048):193–200.

Chan, Ken Y., Min J. Jang, Bryan B. Yoo, Alon Greenbaum, Namita Ravi, Wei Li Wu, Luis Sánchez-Guardado, Carlos Lois, Sarkis K. Mazmanian, Benjamin E. Deverman, and Viviana Gradinaru. 2017. "Engineered AAVs for Efficient Noninvasive Gene Delivery to the Central and Peripheral Nervous Systems." *Nature Neuroscience* 20(8):1172–79.

Chan, Wing Hei, David G. Gonsalvez, Heather M. Young, E. Michelle Southard-Smith, Kylie N. Cane, and Colin R. Anderson. 2016. "Differences in CART Expression and Cell Cycle Behaviour Discriminate Sympathetic Neuroblast from Chromaffin Cell Lineages in Mouse Sympathoadrenal Cells."

Chang, Rui B., David E. Strochlic, Erika K. Williams, Benjamin D. Umans, and Stephen D. Liberles. 2015. "Vagal Sensory Neuron Subtypes That Differentially Control Breathing." *Cell* 161(3):622–33.

Chen, Fuhua, Thomas S. Klitzner, and James N. Weiss. 2006. "Autonomic Regulation of Calcium Cycling in Developing Embryonic Mouse Hearts." *Cell Calcium* 39(5):375–85.

Cheng, Zixi and Terry L. Powley. 2000. "Nucleus Ambiguus Projections to Cardiac Ganglia of Rat Atria: An Anterograde Tracing Study." *Journal of Comparative Neurology* 424(4):588–606.

Cheng, Zixi, Hong Zhang, Shang Z. Guo, Robert Wurster, and David Gozal. 2004. "Differential Control over Postganglionic Neurons in Rat Cardiac Ganglia by NA and DmnX Neurons: Anatomical Evidence." *American Journal of Physiology - Regulatory Integrative and Comparative Physiology* 286(4 55-4):625–33.

Coote, J. H. and R. A. Chauhan. 2016. "The Sympathetic Innervation of the Heart: Important New Insights." *Autonomic Neuroscience: Basic and Clinical* 199:17–23.

Coughlin, Michael D. 1975. "Early Development of Parasympathetic Nerves in the Mouse Submandibular Gland." *Developmental Biology* 43(1):123–39.

D'amico-Martel, Adele and Drew M. Noden. 1983. "Contributions of Placodal and Neural Crest Cells to Avian Cranial Peripheral Ganglia." *American Journal of Anatomy* 166(4):445–68.

D'Autréaux, Fabien, Eva Coppola, Marie Rose Hirsch, Carmen Birchmeier, and Jean François Brunet. 2011. "Homeoprotein Phox2b Commands a Somatic-to-Visceral Switch in Cranial Sensory Pathways." *Proceedings of the National Academy of Sciences of the United States of America* 108(50):20018–23.

Danielian, Paul S., David Muccino, David H. Rowitch, Simon K. Michael, and Andrew P. McMahon. 1998. "Modification of Gene Activity in Mouse Embryos in Utero by a Tamoxifen-Inducible Form of Cre Recombinase." *Current Biology* 8(24):1323–26.

Dauger, Stéphane, Alexandre Pattyn, Frédéric Lofaso, Claude Gaultier, Christo Goridis, Jorge Gallego, and Jean François Brunet. 2003. "Phox2b Controls the Development of Peripheral Chemoreceptors and Afferent Visceral Pathways." *Development* 130(26):6635–42.

Debbache, Julien, Vadims Parfejevs, and Lukas Sommer. 2018. "Cre-Driver Lines Used for Genetic Fate Mapping of Neural Crest Cells in the Mouse: An Overview." *Genesis* 56(6–7).

Desgrange, Audrey, Jean François Le Garrec, and Sigoleѐne M. Meilhac. 2018. "Left-Right Asymmetry in Heart Development and Disease: Forming the Right Loop." *Development (Cambridge)* 145(22).

Desiderio, Simon, Simon Vermeiren, Claude Van Campenhout, Sadia Kricha, Elisa Malki, Sven Richts, Emily V. Fletcher, Thomas Vanwelden, Bela Z. Schmidt, Kristine A. Henningfeld, Tomas Pieler, C. Geoffrey Woods, Vanja Nagy, Catherine Verfaillie, and Eric J. Bellefroid. 2019. "Prdm12 Directs Nociceptive Sensory Neuron Development by Regulating the Expression of the NGF Receptor TrkA." *Cell Reports* 26(13):3522-3536.e5.

Devine, W. Patrick, Joshua D. Wythe, Matthew George, Kazuko Koshiba-Takeuchi, and Benoit G. Bruneau. 2014. "Early Patterning and Specification of Cardiac Progenitors in Gastrulating Mesoderm." *ELife* 3.

Dodou, Evdokia, Michael P. Verzi, Joshua P. Anderson, Shan Mei Xu, and Brian L. Black. 2004. "Mef2c Is a Direct Transcriptional Target of ISL1 and GATA Factors in the Anterior Heart Field during Mouse Embryonic Development." *Development* 131(16):3931–42.

Donocoff, Rachel S., Nato Teteloshvili, Hyunsoo Chung, Rivka Shoulson, and Remi J. Creusot. 2020. “Optimization of Tamoxifen-Induced Cre Activity and Its Effect on Immune Cell Populations.” *Scientific Reports* 10(1):1–12.

Le Douarin, Nicole and Chaya Kalcheim. 2011. “The Autonomic Nervous System and the Endocrine Cells of Neural Crest Origin.” Pp. 197–251 in *The Neural Crest*. Cambridge University Press.

Le Douarin, Nicole M. and Chaya Kalcheim. 1999. *The Neural Crest*.

Dvorakova, Magdalena, Katrin S. Lips, Dörthe Brüggmann, Jana Slavikova, Jitka Kuncova, and Wolfgang Kummer. 2005. “Developmental Changes in the Expression of Nicotinic Acetylcholine Receptor α-Subunits in the Rat Heart.” *Cell and Tissue Research* 319(2):201–9.

Dyachuk, Vyacheslav, Alessandro Furlan, Maryam Khatibi Shahidi, Marcela Giovenco, Nina Kaukua, Chrysoula Konstantinidou, Vassilis Pachnis, Fatima Memic, Ulrika Marklund, Thomas Müller, Carmen Birchmeier, Kaj Fried, Patrik Ernfors, and Igor Adameyko. 2014. “Parasympathetic Neurons Originate from Nerve-Associated Peripheral Glial Progenitors.” *Science* 345(6192):82–87.

Dyck, P., P. Thomas, R. Bunge, and E. Lambert. 2005. *Peripheral Neuropathy*.

Echelard, Yann, Galya Vassileva, and Andrew P. McMahon. 1994. “Cis-Acting Regulatory Sequences Governing Wnt-1 Expression in the Developing Mouse CNS.” *Development* 120(8):2213–24.

Epstein, Douglas J., Michel Vekemans, and Philippe Gros. 1991. “Splotch (Sp2H), a Mutation Affecting Development of the Mouse Neural Tube, Shows a Deletion within the Paired Homeodomain of Pax-3.” *Cell* 67(4):767–74.

Espinosa-Medina, I., E. Outin, C. A. Picard, Z. Chettouh, S. Dymecki, G. G. Consalez, E. Coppola, and J. F. Brunet. 2014. “Parasympathetic Ganglia Derive from Schwann Cell Precursors.” *Science* 345(6192):87–90.

Etchevers, Heather C., Elisabeth Dupin, and Nicole M. Le Douarin. 2019. “The Diverse Neural Crest: From Embryology to Human Pathology.” *Development (Cambridge)* 146(5):0–3.

Förstermann, Ulrich and William C. Sessa. 2012. “Nitric Oxide Synthases: Regulation and Function.” *European Heart Journal* 33(7):829–37.

Fregoso, S. P. and D. B. Hoover. 2012. “Development of Cardiac Parasympathetic Neurons, Glial Cells, and Regional Cholinergic Innervation of the Mouse Heart.” *Neuroscience* 221:28–36.

Furlan, Alessandro and Igor Adameyko. 2018. “Schwann Cell Precursor: A Neural Crest Cell in Disguise?” *Developmental Biology* 444(February):S25–35.

Furlan, Alessandro, Vyacheslav Dyachuk, Maria Eleni Kastriti, Laura Calvo-Enrique, Hind Abdo, Saida Hadjab, Tatiana Chontorotzea, Natalia Akkuratova, Dmitry Usoskin, Dmitry Kamenev, Julian Petersen, Kazunori Sunadome, Fatima Memic, Ulrika Marklund, Kaj Fried, Piotr Topilko, Francois Lallemend, Peter V. Kharchenko, Patrik Ernfors, and Igor Adameyko. 2017. “Multipotent Peripheral Glial Cells Generate Neuroendocrine Cells of the Adrenal Medulla.” *Science* 357(6346).

Glebova, Natalia O. and David D. Ginty. 2004. “Heterogeneous Requirement of NGF for Sympathetic Target Innervation In Vivo.” *Journal of Neuroscience* 24(3):743–51.

Glebova, Natalia O. and David D. Ginty. 2005. “Growth and Survival Signals Controlling Sympathetic Nervous System Development.” *Annual Review of Neuroscience* 28(1):191–222.

Goldgeier, M. H., L. E. Klein, and S. Klein-Angerer. 1984. “The Distribution of Melanocytes in the Leptomeninges of the Human Brain.” *Journal of Investigative Dermatology* 82(3):235–38.

Gonsalvez, David G., Kylie N. Cane, Kerry A. Landman, Hideki Enomoto, Heather M. Young, and Colin R. Anderson. 2013. “Proliferation and Cell Cycle Dynamics in the Developing Stellate Ganglion.” *Journal of Neuroscience* 33(14):5969–79.

Harrington, Anthony W. and David D. Ginty. 2013. “Long-Distance Retrograde Neurotrophic

Factor Signalling in Neurons." *Nature Reviews Neuroscience* 14(3):177–87.
Henning, Robert J. and Darrell R. Sawmiller. 2001. "Vasoactive Intestinal Peptide: Cardiovascular Effects." *Cardiovascular Research* 49(1):27–37.
Hildreth, Victoria, Sandra Webb, Lucy Bradshaw, Nigel A. Brown, Robert H. Anderson, and Deborah J. Henderson. 2008. "Cells Migrating from the Neural Crest Contribute to the Innervation of the Venous Pole of the Heart." *Journal of Anatomy* 212(1):1–11.
Hogan, Niall, Barbara Casadei, and David J. Paterson. 1999. "Nitric Oxide Donors Can Increase Heart Rate Independent of Autonomic Activation." *Journal of Applied Physiology* 87(1):97–103.
Huber, Katrin, Chaya Kalcheim, and Klaus Unsicker. 2009. "The Development of the Chromaffin Cell Lineage from the Neural Crest." *Autonomic Neuroscience: Basic and Clinical* 151(1):10–16.
Isern, Joan, Andrés García-García, Ana M. Martín, Lorena Arranz, Daniel Martín-Pérez, Carlos Torroja, Fátima Sánchez-Cabo, and Simón Méndez-Ferrer. 2014. "The Neural Crest Is a Source of Mesenchymal Stem Cells with Specialized Hematopoietic Stem Cell Niche Function." *ELife* 3:1–28.
Ivanovitch, Kenzo, Susana Temiñ, and Miguel Torres. 2017. "Live Imaging of Heart Tube Development in Mouse Reveals Alternating Phases of Cardiac Differentiation and Morphogenesis."
Jänig, Wilfrid. 2006. *Integrative Action of the Autonomic Nervous System - Neurobiology of Homeostasis*.
Jensen, Bjarke, Tobias Wang, Vincent M. Christoffels, and Antoon F. M. Moorman. 2013. "Evolution and Development of the Building Plan of the Vertebrate Heart." *Biochimica et Biophysica Acta - Molecular Cell Research* 1833(4):783–94.
Jensen, Kristian H. R. and Rune W. Berg. 2016. "CLARITY-Compatible Lipophilic Dyes for Electrode Marking and Neuronal Tracing." *Scientific Reports* 6(May):1–10.
Jessell, Thomas M. 2000. "Neuronal Specification in the Spinal Cord:Inductive Signals and Transcriptional Codes." *Nature Reviews Genetics* 1(October):20–29.
Jessen, Kristjan R. and Rhona Mirsky. 2005. "The Origin and Development of Glial Cells in Peripheral Nerves." *Nature Reviews Neuroscience* 6(9):671–82.
Jessen, Kristjan R. and Rhona Mirsky. 2019. "Schwann Cell Precursors; Multipotent Glial Cells in Embryonic Nerves." *Frontiers in Molecular Neuroscience* 12.
Jiang, Xiaobing, David H. Rowitch, Philippe Soriano, Andrew P. McMahon, and Henry M. Sucov. 2000. "Fate of the Mammalian Cardiac Neural Crest." *Development* 127(8):1607–16.
Kastriti, Maria Eleni and Igor Adameyko. 2017. "Specification, Plasticity and Evolutionary Origin of Peripheral Glial Cells." *Current Opinion in Neurobiology* 47:196–202.
Kastriti, Maria Eleni, Polina Kameneva, Dmitry Kamenev, Viacheslav Dyachuk, Alessandro Furlan, Marek Hampl, Fatima Memic, Ulrika Marklund, Francois Lallemend, Saida Hadjab, Laura Calvo-Enrique, Patrik Ernfors, Kaj Fried, and Igor Adameyko. 2019. "Schwann Cell Precursors Generate the Majority of Chromaffin Cells in Zuckerkandl Organ and Some Sympathetic Neurons in Paraganglia." *Frontiers in Molecular Neuroscience* 12(January):1–18.
Katz, Arnold. 2011. *Physiology of the Heart (Fifth Edition)*.
Kawashima, Tomokazu. 2005. "The Autonomic Nervous System of the Human Heart with Special Reference to Its Origin, Course, and Peripheral Distribution." *Anatomy and Embryology* 209(6):425–38.
Kim, J., L. Lo, E. Dormand, and D. J. Anderson. 2003. "SOX10 Maintains Multipotency and Inhibits Neuronal." *Neuron* 38:17–31.
Kirby, Margaret L. 2007a. "Innervation of the Developing Heart." Pp. 179–98 in *Cardiac Development*.
Kirby, Margaret L. 2007b. "Neural Crest, Great Arteries and Outflow Septation." Pp. 143–60 in

Cardiac Development.
Knox, S. M., I. M. A. Lombaert, X. Reed, L. Vitale-Cross, J. S. Gutkind, and M. P. Hoffman. 2010. "Parasympathetic Innervation Maintains Epithelial Progenitor Cells during Salivary Organogenesis." *Science* 329(5999):1645–47.
Kuhlbrodt, Kirsten, Beate Herbarth, Elisabeth Sock, Irm Hermans-Borgmeyer, and Michael Wegner. 1998. "Sox10, a Novel Transcriptional Modulator in Glial Cells." *Journal of Neuroscience* 18(1):237–50.
Kupari, Jussi, Martin Häring, Eneritz Agirre, Gonçalo Castelo-Branco, and Patrik Ernfors. 2019. "An Atlas of Vagal Sensory Neurons and Their Molecular Specialization." *Cell Reports* 27(8):2508-2523.e4.
Lammert, E., O. Cleaver, and D. Melton. 2001. "Induction of Pancreatic Differentiation by Signals from Blood Vessels." *Science* 294(5542):564–67.
Laughton, W. B. and T. L. Powley. 1987. "Localization of Efferent Function in the Dorsal Motor Nucleus of the Vagus." *American Journal of Physiology - Regulatory Integrative and Comparative Physiology* 252(1 (21/1)).
Lee, Kevin J., Paula Dietrich, and Thomas M. Jessell. 2000. "Genetic Ablation Reveals That the Roof Plate Is Essential for Dorsal Interneuron Specification." *Nature* 403(6771):734–40.
Levin, Mark D., Min Lu Min, Nataliya B. Petrenko, Brian J. Hawkins, Tara H. Gupta, Deborah Lang, Peter T. Buckley, Jeanine Jochems, Fang Liu, Christopher F. Spurney, Li J. Yuan, Jason T. Jacobson, Christopher B. Brown, Li Huang, Friedrich Beermann, Kenneth B. Margulies, Muniswamy Madesh, James H. Eberwine, Jonathan A. Epstein, and Vickas V. Patel. 2009. "Melanocyte-like Cells in the Heart and Pulmonary Veins Contribute to Atrial Arrhythmia Triggers." *Journal of Clinical Investigation* 119(11):3420–36.
Lipp, J. and A. Rudolph. 1972. "Sympathetic Nerve Development in the Rat and Guinea-Pig Heart." *Biol. Neonate* (21):76–82.
Lu, Pengfei and Zena Werb. 2008. "Patterning Mechanisms of Branched Organs." *Science* 322(5907):1506–9.
Markham, Jeffrey A. and James E. Vaughn. 1991. "Migration Patterns of Sympathetic Preganglionic Neurons in Embryonic Rat Spinal Cord." *Journal of Neurobiology* 22(8):811–22.
Marmigère, Frédéric and Patrik Ernfors. 2007. "Specification and Connectivity of Neuronal Subtypes in the Sensory Lineage." *Nature Reviews Neuroscience* 8(2):114–27.
McLean, John H. and David A. Hopkins. 1982. "Ultrastructural Identification of Labeled Neurons in the Dorsal Motor Nucleus of the Vagus Nerve Following Injections of Horseradish Peroxidase into the Vagus Nerve and Brainstem." *Journal of Comparative Neurology* 206(3):243–52.
Metscher, Brian D. 2009. "Micro CT for Comparative Morphology: Simple Staining Methods Allow High-Contrast 3D Imaging of Diverse Non-Mineralized Animal Tissues." *BMC Physiology* 9(1).
Nakamura, Eiichiro, Minh Thanh Nguyen, and Susan Mackem. 2006. "Kinetics of Tamoxifen-Regulated Cre Activity in Mice Using a Cartilage-Specific CreERT to Assay Temporal Activity Windows along the Proximodistal Limb Skeleton." *Developmental Dynamics* 235(9):2603–12.
Nassenstein, Christina, Thomas E. Taylor-Clark, Allen C. Myers, Fei Ru, Rajender Nandigama, Weston Bettner, and Bradley J. Undem. 2010. "Phenotypic Distinctions between Neural Crest and Placodal Derived Vagal C-Fibres in Mouse Lungs." *Journal of Physiology* 588(23):4769–83.
Nedoma, J., J. Slavíková, and S. Tuček. 1986. "Muscarinic Acetylcholine Receptors in the Heart of Rats before and after Birth." *Pflügers Archiv European Journal of Physiology* 406(1):45–50.
Nedvetsky, Pavel I., Elaine Emmerson, Jennifer K. Finley, Andreas Ettinger, Noel Cruz-Pacheco, Jan Prochazka, Candace L. Haddox, Emily Northrup, Craig Hodges, Keith E. Mostov,

Matthew P. Hoffman, and Sarah M. Knox. 2014. “Parasympathetic Innervation Regulates Tubulogenesis in the Developing Salivary Gland.” *Developmental Cell* 30(4):449–62.
Nenasheva, Tatiana A., Marianne Neary, Gregory I. Mashanov, Nigel J. M. Birdsall, Ross A. Breckenridge, and Justin E. Molloy. 2013. “Abundance, Distribution, Mobility and Oligomeric State of M2 Muscarinic Acetylcholine Receptors in Live Cardiac Muscle.” *Journal of Molecular and Cellular Cardiology* 57(1):129–36.
Nitzan, Erez, Elise R. Pfaltzgraff, Patricia A. Labosky, and Chaya Kalcheim. 2013. “Neural Crest and Schwann Cell Progenitor-Derived Melanocytes Are Two Spatially Segregated Populations Similarly Regulated by Foxd3.” *Proceedings of the National Academy of Sciences of the United States of America* 110(31):12709–14.
Pardini, Benet J., Donald D. Lund, and Phillip G. Schmid. 1989. “Organization of the Sympathetic Postganglionic Innervation of the Rat Heart.” *Journal of the Autonomic Nervous System* 28(3):193–201.
Paton, Julian F. R., Sergey Kasparov, and David J. Paterson. 2002. “Nitric Oxide and Autonomic Control of Heart Rate: A Question of Specificity.” *Trends in Neurosciences* 25(12):626–31.
Pattyn, Alexandre, Christo Goridis, and Jean François Brunet. 2000. “Specification of the Central Noradrenergic Phenotype by the Homeobox Gene Phox2b.” *Molecular and Cellular Neurosciences* 15(3):235–43.
Pattyn, Alexandre, Xavier Morin, Harold Cremer, Christo Goridis, and Jean François Brunet. 1997. “Expression and Interactions of the Two Closely Related Homeobox Genes Phox2a and Phox2b during Neurogenesis.” *Development* 124(20):4065–75.
Pattyn, Alexandre, Xavier Morin, Harold Cremer, Christo Goridis, and Jean François Brunet. 1999. “The Homeobox Gene Phox2b Is Essential for the Development of Autonomic Neural Crest Derivatives.” *Nature* 399(6734):366–70.
Pauza, Dainius H., Gertruda Skripkiene, Valdas Skripka, Neringa Pauziene, and Rimvydas Stropus. 1997. “Morphological Study of Neurons in the Nerve Plexus on Heart Base of Rats and Guinea Pigs.” *Journal of the Autonomic Nervous System* 62(1–2):1–12.
Pérez-Pomares, José M., Juan M. González-Rosa, and Ramón Muñoz-Chápuli. 2009. “Building the Vertebrate Heart - An Evolutionary Approach to Cardiac Development.” *International Journal of Developmental Biology* 53(8–10):1427–43.
Petersen, Julian and Igor Adameyko. 2017. “Nerve-Associated Neural Crest: Peripheral Glial Cells Generate Multiple Fates in the Body.” *Current Opinion in Genetics and Development* 45:10–14.
Portbury, Andrea L., Rashmi Chandra, Marybeth Groelle, Michael K. McMillian, Alana Elias, James R. Herlong, Maribel Rios, Suzanne Roffler-Tarlov, and Dona M. Chikaraishi. 2003. “Catecholamines Act via a β-Adrenergic Receptor to Maintain Fetal Heart Rate and Survival.” *American Journal of Physiology - Heart and Circulatory Physiology* 284(6 53-6):2069–77.
Rajendran, Pradeep S., Rosemary C. Challis, Charless C. Fowlkes, Peter Hanna, John D. Tompkins, Maria C. Jordan, Sarah Hiyari, Beth A. Gabris-Weber, Alon Greenbaum, Ken Y. Chan, Benjamin E. Deverman, Heike Münzberg, Jeffrey L. Ardell, Guy Salama, Viviana Gradinaru, and Kalyanam Shivkumar. 2019. “Identification of Peripheral Neural Circuits That Regulate Heart Rate Using Optogenetic and Viral Vector Strategies.” *Nature Communications* 10(1):1–13.
Robinson, B. F., S. E. Epstein, G. D. Beiser, and E. Braunwald. 1966. “Control of Heart Rate by the Autonomic Nervous System. Studies in Man on the Interrelation between Baroreceptor Mechanisms and Exercise.” *Circulation Research* 19(2):400–411.
Rudolph, A. M. 1985. “Distribution and Regulation of Blood Flow in the Fetal and Neonatal Lamb.” *Circulation Research* 57(6):811–21.
Rysevaite, Kristina, Inga Saburkina, Neringa Pauziene, Raimundas Vaitkevicius, Sami F. Noujaim, Jos Jalife, and Dainius H. Pauza. 2011. “Immunohistochemical Characterization of the

Intrinsic Cardiac Neural Plexus in Whole-Mount Mouse Heart Preparations." *Heart Rhythm* 8(5):731–38.

Saga, Yumiko, Sachiko Miyagawa-Tomita, Atsuya Takagi, Satoshi Kitajima, Jun Ichi Miyazaki, and Tohru Inoue. 1999. "MesP1 Is Expressed in the Heart Precursor Cells and Required for the Formation of a Single Heart Tube." *Development* 126(15):3437–47.

Savolainen, SaijaM., Julie F. Foley, and Susan A. Elmore. 2009. "Histology Atlas of the Developing Mouse Heart." *Toxicologic Pathology* 37(4):395–414.

Schindelin, Johannes, Ignacio Arganda-Carreras, Erwin Frise, Verena Kaynig, Mark Longair, Tobias Pietzsch, Stephan Preibisch, Curtis Rueden, Stephan Saalfeld, Benjamin Schmid, Jean Yves Tinevez, Daniel James White, Volker Hartenstein, Kevin Eliceiri, Pavel Tomancak, and Albert Cardona. 2012. "Fiji: An Open-Source Platform for Biological-Image Analysis." *Nature Methods* 9(7):676–82.

Shefa, Ulfuara, Dokyoung Kim, Min Sik Kim, Na Young Jeong, and Junyang Jung. 2018. "Roles of Gasotransmitters in Synaptic Plasticity and Neuropsychiatric Conditions." *Neural Plasticity* 2018.

Shigenobu, K., H. Tanaka, and Y. Kasuya. 1988. "Changes in Sensitivity of Rat Heart to Norepinephrine and Isoproterenol during Pre- and Postnatal Development and Its Relation to Sympathetic Innervation." *Developmental Pharmacology and Therapeutics* 11(4):226–36.

Soldatov, Ruslan, Marketa Kaucka, Maria Eleni Kastriti, Julian Petersen, Tatiana Chontorotzea, Lukas Englmaier, Natalia Akkuratova, Yunshi Yang, Martin Häring, Viacheslav Dyachuk, Christoph Bock, Matthias Farlik, Michael L. Piacentino, Franck Boismoreau, Markus M. Hilscher, Chika Yokota, Xiaoyan Qian, Mats Nilsson, Marianne E. Bronner, Laura Croci, Wen Yu Hsiao, David A. Guertin, Jean Francois Brunet, Gian Giacomo Consalez, Patrik Ernfors, Kaj Fried, Peter V. Kharchenko, and Igor Adameyko. 2019. "Spatiotemporal Structure of Cell Fate Decisions in Murine Neural Crest." *Science* 364(6444).

Soriano, Philippe. 1999. "Generalized LacZ Expression with the ROSA26 Cre Reporter Strain." *Nature* 21(january):70–71.

Steel, K. P. and C. Barkway. 1989. "Another Role for Melanocytes: Their Importance for Normal Stria Vascularis Development in the Mammalian Inner Ear." *Development* 107(3):453–63.

Takeuchi, Jun K., Makoto Ohgi, Kazuko Koshiba-Takeuchi, Hidetaka Shiratori, Ichiro Sakaki, Keiko Ogura, Yukio Saijoh, and Toshihiko Ogura. 2003. "Tbx5 Specifies the Left/Right Ventricles and Ventricular Septum Position during Cardiogenesis." *Development* 130(24):5953–64.

Thaler, Joshua P., Sonya J. Koo, Artur Kania, Karen Lettieri, Shane Andrews, Christopher Cox, Thomas M. Jessell, and Samuel L. Pfaff. 2004. "A Postmitotic Role for Isl-Class LIM Homeodomain Proteins in the Assignment of Visceral Spinal Motor Neuron Identity." *Neuron* 41(3):337–50.

Thomas, Steven A., Alvin M. Matsumotot, and Richard D. Palmiter. 1995. "Noradrenaline Is Essential for Mouse Fetal Development." 374(April):643–46.

Tsai, William, Anthony D. Morielli, and Ernest G. Peralta. 1997. "The M1 Muscarinic Acetylcholine Receptor Transactivates the EGF Receptor to Modulate Ion Channel Activity." *EMBO Journal* 16(15):4597–4605.

Van Vliet, Kim M., Veronique Blouin, Nicole Brument, Mavis Agbandje-McKenna, and Richard O. Snyder. 2008. "The Role of the Adeno-Associated Virus Capsid in Gene Transfer." *Methods in Molecular Biology* 437:51–91.

Wang, Jingya, Marian Kollarik, Fei Ru, Hui Sun, Benjamin McNeil, Xinzhong Dong, Geoffrey Stephens, Susana Korolevich, Philip Brohawn, Roland Kolbeck, and Bradley Undem. 2017. "Distinct and Common Expression of Receptors for Inflammatory Mediators in Vagal Nodose versus Jugular Capsaicin-Sensitive/TRPV1-Positive Neurons Detected by Low Input RNA Sequencing." *PLoS ONE* 12(10):1–20.

Wang, Liang, Alessandro Mongera, Dario Bonanomi, Lukas Cyganek, Samuel L. Pfaff, Christiane

Nüsslein-Volhard, and Till Marquardt. 2014. “A Conserved Axon Type Hierarchy Governing Peripheral Nerve Assembly.” *Development (Cambridge)* 141(9):1875–83.
Wang, Qi, Hiroshi Kurosaka, Masataka Kikuchi, Akihiro Nakaya, Paul A. Trainor, and Takashi Yamashiro. 2019. “Perturbed Development of Cranial Neural Crest Cells in Association with Reduced Sonic Hedgehog Signaling Underlies the Pathogenesis of Retinoic-Acid-Induced Cleft Palate.” *Disease Models & Mechanisms* 12(10):dmm040279.
Wildenthal, K. 1973. “Maturation of Responsiveness to Cardioactive Drugs. Differential Effects of Acetylcholine, Norepinephrine, Theophylline, Tyramine, Glucagon, and Dibutyryl Cyclic AMP on Atrial Rate in Hearts of Fetal Mice.” *Journal of Clinical Investigation* 52(9):2250–58.
Wilkinson, David G., Juliet A. Bailes, and Andrew P. McMahon. 1987. “Expression of the Proto-Oncogene Int-1 Is Restricted to Specific Neural Cells in the Developing Mouse Embryo.” *Cell* 50(1):79–88.
Woods, Stephen C. and Daniel Jr. Porte. 1974. “Neural Control of the Endocrine Pancreas.” *Best Practice and Research: Clinical Endocrinology and Metabolism* 54(3).
Yamagishi, Hiroyuki. 2020. “Cardiac Neural Crest.” *Cold Spring Harbor Perspectives in Biology* a036715.
Yang, Baofeng, Huixian Lin, Chaoqian Xu, Yan Liu, Huizhen Wang, Hong Han, and Zhiguo Wang. 2005. “Choline Produces Cytoprotective Effects against Ischemic Myocardial Injuries: Evidence for the Role of Cardiac M 3 Subtype Muscarinic Acetylcholine Receptors.” *Cellular Physiology and Biochemistry* 16(4–6):163–74.
Yang, Guang, Cora Sau, Wan Lai, Joseph Cichon, and Wei Li. 2008. “A Central Role for Islet1 in Sensory Neuron Development Linking Sensory and Spinal Gene Regulatory Programs.” *Nature Neuroscience*.
Yang, Xia, Silvia Arber, Christopher William, Li Li, Yasuto Tanabe, Thomas M. Jessell, Carmen Birchmeier, and Steven J. Burden. 2001. “Patterning of Muscle Acetylcholine Receptor Gene Expression in the Absence of Motor Innervation.” *Neuron* 30(2):399–410.
Yuan, Hsiangkuo and Stephen D. Silberstein. 2016. “Vagus Nerve and Vagus Nerve Stimulation, a Comprehensive Review: Part I.” *Headache* 56(1):71–78.
Zhou, Qun Yong, Carol J. Quaife, and Richard D. Palmiter. 1995. “Targeted Disruption of the Tyrosine Hydroxylase Gene Reveals That Catecholamines Are Required for Mouse Fetal Development.” 374(April):640–43.
Zucker, Irving H., Harold D. Schultz, Yi Fan Li, Yu Wang, Wei Wang, and Kaushik P. Patel. 2004. “The Origin of Sympathetic Outflow in Heart Failure: The Roles of Angiotensin II and Nitric Oxide.” *Progress in Biophysics and Molecular Biology* 84(2–3):217–32.
van Zwieten, P. A. and H. N. Doods. 1995. “Muscarinic Receptors and Drugs in Cardiovascular Medicine.” *Cardiovascular Drugs and Therapy* 9(1):159–67.

Eurexpress - A Transcriptome Atlas Database for Mouse Embryo
CHRNA4 in E14.5 mouse embryo
http://www.eurexpress.org/ee/databases/assay.jsp?assayID=euxassay_017932&image=01
)

Allen Brain Atlas – *Chrna4* in E13.5 and E15.5 mouse embryo
© 2008 Allen Institute for Brain Science. Allen Developing Mouse Brain Atlas. Available from:
https://developingmouse.brain-map.org/experiment/show/100042359
https://developingmouse.brain-map.org/experiment/show/100042441

Images from external sources:

Histological sagittal section of E13.5 mouse embryo:
eHistology Atlas (http://www.emouseatlas.org/emap/eHistology/)

Graham E, Moss J, Burton N, Roochun Y, Armit C, Richardson L and Baldock R (2015) The atlas of mouse development eHistology resource. Development. 142:1909-1911. doi: 10.1242/dev.124917 (emouseatlas.org/eAtlasViewer_ema/application/ema/kaufman/plate_31a.php?image=a)

Science. Allen Developing Mouse Brain Atlas. Available from: developingmouse.brain-map.org
Prdm12 in situ detection in E13.5:
https://developingmouse.brain-map.org/experiment/show/113116439

Science. Allen Developing Mouse Brain Atlas. Available from: developingmouse.brain-map.org
Phox2b in situ detection in E13.5:
https://developingmouse.brain-map.org/experiment/show/100053254

Supplementary

3D animations of segmented embryonic heart

Three-dimensional reconstruction and short animations of embryonic hearts were created with 3D Visualization & Analysis Software Amira-Avizo (ThermoFisher™). The animations can be accessed via the following link:

https://drive.google.com/drive/folders/1QEvO1J8vmSRSGTSnKUG0Z8zck0Km1WF1?usp=sharing

Abbreviations

AA	aortic arch
AAo	ascending aorta
ACh	Acetylcholine
AM	adrenal medulla
ANS	autonomic nervous system
Ao	aortic trunk
AS	aortic sac
AVL	aortic valve leaflet
cAMP	cyclic adenosine monophosphate
cANS	cardiac autonomic nervous system
ChAT	choline acetyltransferase
CNCC	cardiac neural crest cell
CPG	cardiac paraganglia
CTB	cholera toxin subunit B
DAo	descending aorta
DBH	dopamine β-hydroxylase
ddH_2O	double-distilled water
DmnX	dorsal motor nucleus of the vagus
DRG	dorsal root ganglia
DTA	diphtheria toxin
E9.5	embryonic day 9.5
EGF	epidermal growth factor
EGFR	epidermal growth factor receptor
EtOH	ethanol
FHF	first heart field
HCR	hybridization chain reaction
IVC	inferior vena cava
IVS	interventricular septum
JG	jugular ganglion
LA	left atrium
LDAo	left dorsal aorta
LV	left ventricle
M1	muscarinic receptor 1
MeOH	methanol
microCT	micro computer tomography
MN	motor neuron
NA	nucleus ambiguus
NC	neural crest
NCC	neural crest cell
NE	norepinephrine (noradrenaline)
NG	nodose ganglion
NGF	nerve growth factor
NO	nitric oxide
nX	vagal nerve

OCT	optimal cutting temperature compound
Oe	oesophagus
OFT	outflow tract
OV	otic vesicle
PA	pulmonary artery
PBr	primary bronchus
PBS	phosphate-buffered saline
PBST	phosphate-buffered saline with Tween
PFA	paraformaldehyde
PKA	protein kinase A
PNS	peripheral nervous system
PSG	Parasymp. submandibular ganglion
PT	pulmonary trunk
PTA	phosphotungstic acid
RDAo	right dorsal aorta
RT	room temperature
SC	sympathetic chain
SCC	saline-sodium citrate
SCG	sympathetic chain ganglion
SCP	Schwann cell precursor
SHF	second heart field
SMG	submandibular gland
T	trachea
TAM	tamoxifen
TF	transcription factor
TG	trigeminal ganglion
TGF-a	transforming growth factor-a
TH	tyrosin hydroxylase
TrkA	tropomyosin receptor kinase
VAChT	vesicular acetylcholine transporter
VIP	vasoactive intestinal peptide
VIPR1	vasoactive intestinal peptide receptor 1
YFP	yellow flourescent protein
ZO	Zuckerkandl organ